1-1-2013

Representing Intersubject Variability with a Statistical Shape and Alignment Model of the Knee

Chandreshwar Rao
University of Denver

Representing Intersubject Variability with a Statistical Shape and Alignment Model of the Knee

Abstract

Prior statistical shape models have not considered multiple structures in the knee joint to characterize anatomic variation which are required to investigate joint mechanics further for the successful knee replacement. Accordingly, the study's objective was to develop statistical shape and alignment model (SSAM) to capture intersubject variability and demonstrate the ability to generate realistic instances for use in finite element analysis (FEA). SSAM described the variability in the training set of 20 subjects with a series of modes of variation obtained by performing principal component analysis (PCA). PCA produced modes of variation with the first 3 modes representing 70% and 10 modes representing 95% variability when only bones of the joint were studied. Modes were perturbed by ± 2ó and computational models of new virtual subjects were generated. FEA successfully confirmed the fidelity of the SSAM approach. The relationship between SSAM and function (motion) were investigated through the shape-function model. The framework can create new subject and predict the kinematic behavior. The approach can be an investigative tool to differentiate in the shape-function relation between healthy normal and pathologic groups.

Document Type

Thesis

Degree Name

M.S.

Department

Mechanical Engineering

First Advisor

Peter J. Laz, Ph.D.

Second Advisor

Paul Rullkoetter

Third Advisor

Alvaro Arias

Keywords

Customized implant, Finite element analysis, Kinematics predictions, Knee joint, Population-based variability, Statistical shape model

Subject Categories

Biomedical Engineering and Bioengineering | Mechanical Engineering

REPRESENTING INTERSUBJECT VARIABILITY WITH A STATISTICAL SHAPE AND ALIGNMENT MODEL OF THE KNEE

A Thesis

Presented to

the Faculty of Engineering and Computer Science

University of Denver

In Partial Fulfillment

of the Requirements for the Degree

Master of Science

---

by

Chandreshwar Rao

March 2013

Advisor: Peter J. Laz

Author: Chandreshwar Rao
Title: REPRESENTING INTERSUBJECT VARIABILITY WITH A STATISTICAL SHAPE AND ALIGNMENT MODEL OF THE KNEE
Advisor: Peter J. Laz
Degree Date: March 2013

ABSTRACT

Prior statistical shape models have not considered multiple structures in the knee joint to characterize anatomic variations which are required to investigate joint mechanics further for the successful knee replacement. Accordingly, the study's objective was to develop statistical shape and alignment model (SSAM) to capture intersubject variability and demonstrate the ability to generate realistic instances for use in finite element analysis (FEA). SSAM described the variability in the training set of 20 subjects with a series of modes of variation obtained by performing principal component analysis (PCA). PCA produced modes of variation with the first 3 modes representing 70% and 10 modes representing 95% variability when only bones of the joint were studied. Modes were perturbed by $\pm 2\sigma$ and computational models of new virtual subjects were generated. FEA successfully confirmed the fidelity of the SSAM approach. The relationship between SSAM and function (motion) were investigated through the shape-function model. The framework can create new subject and predict the kinematic behavior. The approach can be an investigative tool to differentiate in the shape-function relation between healthy normal and pathologic groups.

ACKNOWLEDGEMENTS

First, to my advisor, Dr. Peter Laz, thank you for your support and exact guidance. It was a great experience to learn under your mentorship. Thank you for your kindness in allowing me to stay at your house for a couple of weeks before I found an apartment for my family. I also want to thank my committee members, Dr. Paul Rullkoeter and Dr. Alvaro Arias. Dr. Rullkoeter, your FEA work on knees motivated me to study at DU. Dr. Arias, thank you for graciously agreeing to be the external chairperson on short notice. Thank you to every member of the computational biomechanics labs, in particular, Kevin, Clare, Brad, Milind, Chadd, Abe, Sean, Tariq, Steven, James, Azhar, for your every help. Special thanks to Renee from the Engineering Office for your very timely support with paper work. To the folks at KU, thank you for providing knee simulator data for this study.

I would like to thank my Indiana neighbors, Mark and Lisa, for your support and encouragement, and for proofreading the chapters of my thesis. Your endless love and affection for my family make us feel home in the USA.

I would to thank my wife, Suchita, and daughter, Advika, for your unending support throughout the study. I love you both. I want to thank my family in India (parents, in-laws and younger brother, Priyaranjan) for your love and encouragement. I dedicate this work to you all.

Lastly, thanks to the National Science Foundation because without your funding, this research would not have been possible.

TABLE OF CONTENTS

LIST OF FIGURES

Page

LIST OF TABLES

Page

CHAPTER 1 – INTRODUCTION

1.1 Background

Performance of orthopaedic implants varies dramatically between subjects because of natural intersubject variability and surgical skill. However, natural intersubject variability is ignored and the majority of studies use a single or limited number of bone models [Bryan et al., 2010]. Therefore, it is vital to consider intersubject variability. Intersubject variability is inherently present in bone quality, patient anatomy, and representation of both variation in shape and relative alignment of the articular geometry [Laz and Browne, 2010; Bryan et al., 2010].

Computed tomography (CT) and magnetic resonance (MR) images, at present, are the method of choice for the generation of subject-specific models. It has made it possible to define the geometry and the local tissue properties of the bone segment to be modeled [Taddei et al., 2006]. Increasing availability of imaging techniques provide information to diagnose pathologies (e.g. patellar maltracking, cartilage degradation, joint laxity, etc.) and also help understand variability in patient anatomy. Subject-specific anatomy consideration is becoming popular in designing customized instruments and implants, and in making surgical decisions. So, understanding the variability associated

with anatomy and alignment has a larger role to play in the future in pathologies diagnosis, surgical procedures, and the development of customized and robust implants for patient care. Recently, hip resurfacing implants were recalled due to concern over their robustness to malalginment. Capturing subject-specific anatomy and alignment variability and then integrating that with kinematic predictions will be useful to understand the variability in the joint mechanics. For example, patellofemoral pain has been related to abnormal PF kinematics [Fizpatrick et al., 2011].

Statistical shape models have been widely used to characterize variability of a population data set and in predicting a new instance among that population. Particularly in orthopaedics domain, shape models have been applied to characterize variability in the bone morphology for training sets of subjects representing the population; for example, in the femur [Bryan et al., 2010; Bredbenner et al., 2008], pelvis [Meller and Kalender, 2004] and shoulder [Yang et al., 2008]. Variability in the bone material density along with bone morphology has also been studied [Bryan et al., 2010; Fritscher et al., 2009]. Statistical shape models use a point distribution model to establish point-to-point correspondence between the instances in a training set [Cootes et al., 1995; Meller and Kalender, 2004; Behiels et al., 2002].

Principal component analysis is a method to describe the variability in the set of corresponding points with a series of common modes of variation. It provides amount and direction of change information [Jolliffe, 2002] which has ability to characterize the variability in the data. It has benefits in 1) variability quantification, 2) predicting new virtual geometries (based on the prior population data) with direct application in finite

element analysis, and 3) efficiently predicting a subject-specific representation from incomplete or sparse data sets from less invasive methods (e.g. ultrasound) [Barratt et al., 2008; Shim et al., 2008; Rajamani et al., 2007].

So far, shape models have focused on individual bones which can provide benefits like development of implant sizing lines [Fitzpatrick et al., 2007] or the evaluation of bone fracture risk because of shape and material properties inclusion together [Bryan et al., 2010; Fritscher et al., 2009]. Quantitative differences in femur and tibia surface geometry have been characterized through shape models to distinguish between two groups who are not expected to develop osteoarthritis [Bredbenner et al., 2010]. Patello-femoral joint has been also studied utilizing shape model approach [Baldwin et al., 2010].

Eventually, in order to utilize statistical models in evaluations of joint mechanics (patellofemoral as well as tibiofemoral), the statistical model must consider all important structures comprising the joint, their interdependencies and their relative alignment. A complete knee statistical shape model can be comprised of all major bones (femur, tibia, and patella), major cartilages (femoral, tibial-medial, tibial-lateral, and patellar), major ligaments (medial-collateral, lateral-collateral, posterior-cruciate, and anterior-cruciate). In this way, the statistical model will preserve common changes in shape between structures, such as the influence of size across the femur, tibia and patella, or the mirroring of the shape of the patella and the trochlear groove of the femur. In addition, the relative alignment of the structures will be preserved, which influence a subject's joint mechanics. [Baldwin et al., 2010; Fizpatrick et al., 2011; Bredbenner et al, 2010].

Previous shape models have considered the relative position of structures by using global scan space coordinates, but this does not discriminate between differences in anatomic alignment and artifacts resulting from differences in the scanned position (knee flexed slightly or internally rotates). Choosing a known flexion where quadriceps is loaded for relative alignment of bones can rule out limitations of the scanned position. So, this study focuses on developing statistical shape models for characterizing shape and alignment variability of the complete knee joint from a population data set. Application of shape models will be demonstrated by generating new subjects, and performing finite element analysis for contact mechanics, and characterizing relationship with function-kinematics.

1.2 Motivation

Knee osteoarthritis (OA) affects millions of people worldwide. In most cases, loss of cartilage in the joints happens due to aging and causes activity limitation in older age groups [http://oai.epi-ucsf.org]. OA is the most prominent cause for total knee replacement (TKR), an ultimate solution to treat the affected knee and again restore the motion of the knee.

Success of TKR depends on the resultant post-operative knee joint mechanics which should be reasonably close to natural knee joint mechanics. Therefore, it becomes necessary to understand knee joint mechanics which can results in better inputs for implant design. Knee joint mechanics are subject-specific and clinical and in-vitro studies report significant levels of intersubject variability in terms of kinematics, joint

loading, knee structures and bone and soft tissues material properties. Most importantly, anatomical variation is the main contributor to intersubject joint mechanics variability. Hence, to achieve a successful TKR, it is necessary to characterize the intersubject variability and use those characteristics for implant design.

Due to technological advancement, the standard process to develop a subject-specific model is to reconstruct bony structures along with soft tissues from CT or MR images. However, adopting this process for subject-specific model is a labor intensive and time consuming process. On the other hand, from a training set across population, using statistical shape model (SSM) more realistic subject specific model prediction can be achieved in shorter time. Recently, SSM have characterized bony morphology and have included shape and intensity representing density and material property variability [Bryan et al., 2010; Fritscher et al., 2009]. Statistical shape models have applications to population-based evaluations (e.g. osteoarthritis [Bredbenner et al., 2010]) and in the efficient development of subject-specific models from a subset of measurements [Rajamani et al., 2007]. Statistical shape models have the potential to represent a population-based model and efficiently generate subject-specific model for surgical planning through computer assisted surgery. Previous studies of statistical shape modeling have focused on the partial structure of a joint and have limited application. But applying this approach to a joint consisting of bones, cartilage, ligaments and other structures will have many clinical applications in population-based customized treatment of OA. Moreover, representing the variability of the complete knee joint which has a higher degree of complexity through SSM is more challenging. It requires not only

registration of the structures of the knees in the training set but also preservation of relative position of the structures, a challenging task. Inclusions of ligaments surrounding the knee which provide unique motion constraint have heavy influence to the knee mechanics. As knee mechanics is important for the proper mobility of the subject, it becomes important to account for the ligament attachment variability (inter-subject variability) and hence develop a robust SSAM model for patient's surgical need and ensuring success of TKR. This thought was motivational in applying SSM concept to a challenging situation like representing a joint that contains bones, cartilages and ligaments, and then characterizing the intersubject variability, and demonstrating the ability to generate new virtual subjects for use in finite element analysis and TKR implant design, will be useful with many clinical applications.

There are other potential areas where further research is required. SSAM can also be utilized in conjunction with correlated anatomical measurement (e.g. femoral epicondyles distance, femoral radius) to predict accurate patient's specific geometry for pre-operating planning and surgical decisions like identifying mechanical axes, bone cut, component sizing, and placement. It could greatly drive patient’s specific customized implants manufacturing and hence would serve patient's specific need rather than available standard size implants.

1.3 Objectives

As discussed above, statistical shape models have the potential to generate subject-specific models from a population and help assist surgeons for surgical planning

through computer assisted surgery. Furthermore, statistical shape model can be used in computational analysis to simulate natural and implanted joint mechanics, and then evaluate the robustness of implants design. Accordingly, the sequential objectives of this study were:

-To develop an approach to represent a population-based intersubject variability in bone morphology and soft issues and alignment for the structures of the knee through statistical shape and alignment modeling (SSAM).

-To demonstrate the ability of statistical models to describe variability in a training set and to generate realistic instances for use finite element (FE) analysis related to joint mechanics.

-To apply statistical modeling approach to characterize relationships between shape, alignment and kinematics (motions) through the shape-function model

Moreover, this study will also advance prior statistical shape modeling efforts [Baldwin et al., 2010] (Figure 2.10) by isolating the shape and alignment components of the variability and reporting alignments in a kinematic form relative to anatomical reference frames for a controlled knee position (30^0 flexion). A controlled position was chosen to avoid capturing variability because of uncontrolled and unloaded scan position. If scan position would have been taken then it will be difficult to differentiate whether the variability observed is due to relative alignment of knee structures or differences in the scan position. The larger aim of this study is to produce statistical shape models in FE model format. This approach will enable the joint mechanics assessments because of the influence of the shape and alignment by evaluating contact mechanics and kinematics for

a perturbed shape model (representing a new subject). Moreover, the FE model is also useful for pathological investigation, like patellar mal tracking and patellofemoral pain [Fitzpatrick et al., 2011], and robust implant design evaluation with a population of subjects.

1.4 Organization

Chapter 2 consists of literature review, which provides information about basic anatomy of the human knee joint relevant to statistical shape models and prior statistical shape models and principal component analysis.

Chapter 3 provides the information of software tools used, methods and procedures followed to develop training set data, and statistical method to develop statistical shape models. This Chapter has three different cases: bones only, bones and cartilages, and bones and cartilages and ligaments of statistical shape modeling. These cases are with increasing complexity.

Chapter 4 presents the results and analysis of the results for all three different cases of SSAM. It also discusses the fidelity of the SSAM through running a finite element analysis and presenting the results.

Chapter 5 is dedicated to the demonstrated application of SSAM. In this chapter, a developed framework for knee kinematics prediction for the new virtual subject is discussed.

Chapter 6 concludes the dissertation by highlighting the results and making recommendations for future work in the field of study.

CHAPTER 2 – LITERATURE REVIEW

This chapter provides literature review on general background of clinical terminologies, human knee anatomy, prior statistical shape models, and principal component analysis.

2.1 Clinical Terminology

In human anatomy, a well- defined terminology is extremely useful for the consistent description of the relative motions of the human body. Relative motions of the body have been described with the help of three anatomical planes: sagittal, coronal (frontal), and transverse (axial). These three planes are based on positions relative to the body in standing position with arms at the side and palms facing forwards (Figure 2.1). The sagittal plane divides the body into right and left halves from head to toe. A structure is said to be medial to another if it is closer to the midline and lateral if it is further away. The coronal or frontal plane is perpendicular to the sagittal plane, bisecting the body into front and back halves and a structure is described to be anterior if it is nearer to the front of the body and posterior if it is closer to the back. The transverse or horizontal plane intersects the body at right angles to the sagittal and coronal planes, parallel to the ground and divides the body into superior (head) and inferior (toe) sections. A structure is superior if it is at a higher level or closer to the head and inferior

if it is at a lower level or away from the head. Additionally, the terms proximal and distal may be used to indicate an object is closer to the center of the body (proximal) or farther away from the body center (distal) (Figure 2.2). Six terminologies: anterior-posterior, medial-lateral, inferior-superior, flexion-extension, internal-external and varus-valgus are used to describe six degrees of freedom to define the relative motion of the knee joint and have been used in this study. The first three are for three translational degrees of freedom of the knee while the next three are for three rotational degrees of freedom (Figure 2.3). Flexion is a movement in the sagittal plane reducing the angle between the femur and the tibia, while extension is the increase in angle between the two bones. An internal rotation occurs about the inferior-superior axis when one bone rotates toward the midline of the body, and an external rotation occurs when the bone rotates away from the midline. An adduction (varus) is the movement toward the midline in the coronal plane while abduction (valgus) is the movement away.

2.2 Anatomy of the Human Knee

This review of the literature is focused on important structures (bones and soft-tissues) of the human knee joint that influence its functional behavior most and relevant to the subject of this study. Functional behavior is controlled by mainly articular surfaces, ligaments, and tendons at the knee joints. The articular surfaces of the knee are located on the three bony structures: distal end of femur, proximal end of tibia, and posterior face of patella (Figure 2.4). The femur to the tibia articulation occurs at the tibiofemoral or knee joint, and the femur and the patella articulation happens at the patellofemoral joint.

At the knee, the articular surface of the tibiofemoral and patellofemoral joints are covered in a thin layer of highly organized tissue comprised of collagen and elastin fibers known as articular cartilage (Figure 2.5). The articular surface of tibiofemoral consists of the medial and lateral femoral condyles, sulcus groove, the posterior aspect of the patella and the proximal tibial surface (Figure 2.6). The primary functions of the articular cartilage are to decrease contact stresses by distributing loads over a wide area, and to permit relative movement of the opposing joint surfaces with low coefficient of friction of around $\mu = 0.01$ [Ramakrishnan et al., 2001] at the joint. Over time, depending upon activities and age, the articular cartilage can wear away and exposes the rough bones in direct contact and cause knee pain and restricted knee activities (known as osteoarthritis). These degenerated articulating surfaces are removed during total knee arthroplasty.

The stability of the knee joint is provided by an extensive network of ligaments and tendons around the knee joint. Ligaments are bands of strong fibrous connective tissue that fasten together the articular ends of bones and cartilage at the joints to provide passive constraint to the knee. A majority of this constraint is provided by four major ligaments: the anterior and posterior cruciate ligaments (ACL and PCL) and the medial and lateral collateral ligaments (MCL and LCL) (Figure 2.5). The ACL and PCL prevent sliding of the tibia in the anterior and posterior directions, respectively. The collateral ligaments provide medial-lateral and varus-valgus stability, and limit internal-external rotation during extension.

The three bones listed above (femur, tibia and patella), and their respective cartilages, and the attachment sites of four ligaments have been considered in the shape

and alignment modelling. Detailed attachment sites of MCL have been shown in Figure 2.7. As in, MCL has three prominent attachment sites- femoral, proximal tibial and distal tibial. Additionally, from a cadaveric specimen the location of MCL and LCL in deep knee flexion has been shown in Figure 2.8.

2.3 Statistical Shape Modeling

In the past, SSM was typically used to investigate individual bone but, have not considered multiple structures in a joint that would be required to assess the complete joint mechanics. Numerous studies have investigated relationships between shape of the articular geometry and joint mechanics, for example in the patellofemoral joint [Fitzpatrick et al., 2011]. Recently, three dimensional statistical shape models of the femur for finite element analysis have been created. These models also characterized shape and intensity representing density and material property variability [Bryan et al., 2010]. The variation in both geometry and material properties were extracted from computer tomography (CT) scans and statistical shape models captured that information. Similarly, three dimensional statistical shape models of the tibia for finite element analysis have been created [Galloway et al., 2012] (Figure 2.9).

In another study [Fritscher et al., 2009], shape and spatial intensity distribution of the femur were combined and the inner structure of the proximal femur was analyzed to predict a biomechanical parameter using appearance statistical models developed from CT and X-ray images. Based on this study, using an automated approach, accurate predictions of the bone mineral density and biomechanical properties were achieved,

which otherwise would have been inappropriate using conventional methods, such as a surgeon's experience. To summarize, statistical shape models have important application in the accurate prediction of bone parameters.

SSM also helps assist treatment of knee OA, and provides a mean to describe spatial variation in joint surface geometry between healthy subjects and those with clinical risk of developing osteoarthritis [Bredbenner et al., 2010]. It has been demonstrated that SSM is capable of efficiently describing the quantitative differences in tibia and femur articulating geometry. The study is comprised of two bones of the knee joint without considering other structures present in the knee joint. Notably, the study substantiated that SSM has application in OA treatment and how the SSM could be used to differentiate between patients who are not expected to develop OA and those who are at the clinical risk of OA. This proven application of SSM developed from just two bones, i.e. femur and tibia, guides the path forward to develop SSM from all structures of the knee.

Another study [Rajamani et al., 2007] has described 3-D model construction by fitting statistical deformable model to minimal sparse 3D data consisting of digitized landmarks and surface that are obtained intra-operatively. It presented a novel anatomical shape deformation technique, operated on sparse sets of surface points and also on small and large sets of digitized points using point distribution model (PDM).

A more recent study [Fitzpatrick et al., 2011] investigated the relationship between statistical shape models and joint mechanics. Probabilistic analyses were combined with statistical shape model to predict patellofemoral joint mechanics. This

approach was helpful to deal with difficult sensitivity analysis on a larger number of parameters. In the combined probabilistic and statistical shape approach, first probabilistic (Monte Carlo) analysis was used on variable parameters to create a training set and then statistical shape model development technique was applied to investigate variability. It was applied in biomechanical analysis to characterize the effect of implant alignment and loading on the patellofemoral joint mechanics in the TKR. Though this study focused on only patellofemoral joint mechanics, tibiofemoral joint mechanics inclusion could be the path forward to complete representation of knee joint mechanics. In the above studies, SSM concepts have been appreciably used to characterize the variability in the data set and their usages.

The methods for developing a statistical shape model are standardized and consist of two main steps:

1. Establishing nodal correspondence in the training set, and
2. Performing principal component analysis, *discussed in next section*

First, and the most important step, in SSM development is establishing accurate node to node correspondence between instances in the training set so that realistic representation of shape is feasible. The training set geometries are defined by a set of points or nodes representing the surfaces of the structures and the statistical shape model then characterize the changes in the location of the nodes for the specimens in the training set. Commonly, iterative closet point (ICP) algorithms, also called registration algorithm, are used for nodal correspondence. ICP requires procedures to find the closest on the geometric entity to a given point. A general purpose method for registration of 3-

D shape [Besl et al., 1992] describes that ICP has capabilities to register point sets, curves and surfaces. However, ICP works on best initial guess of matching specially rotation and sometime noise level could be very large and results in gross statistical outliers, also complex geometries are sometimes computationally expensive. The point distribution technique (PDM) has also been used for nodal correspondence in the past [Rajamani et al., 2007]. PDM technique defines handles corresponding to anatomical landmark locations, including bony features, prominences, etc. on the segmented geometry of each subject in the training set. Integrated mesh-morphing-based segmentation approach was another technique, recently developed by [Baldwin et al., 2010] to create hexahedral meshes (3D) of subject-specific scan data. This method integrated segmentation of a structure in a scan image to nodes in the template mesh. The template mesh was the same for a particular structure and nodal correspondence was well established. This was a computationally efficient method as it avoided one intermediate step of time consuming 3D meshing. This approach created FE based statistical shape models for uncontrolled and unloaded scan position (Figure 2.10).

Hexahedral meshing is more realistic for deformable structures like cartilages for accurate finite element analysis (FEA) results. Therefore, developing SSM from 3D mesh will have direct application in FEA.

Additionally, intersubject variability has not been assessed to multiple source of variability like material properties, TKR design and alignment and then predicting joint mechanics. So, there is scope for further research to investigate the influence of material properties and TKR implant alignment variability in conjunction with geometric

variability of the knee to predict bounds of performance of joint mechanics for a population.

2.4 Principal Component Analysis

The second step in the development of statistical shape model is principal component analysis (PCA). PCA is a multivariate statistical technique for simplifying complex data sets. It reduces the dimensionality of a multivariate data set while retaining as much variation as possible [Jolliffe, 2002]. The goal of PCA is to find new lesser key variables termed as principal components (PCs) [Raychaudhuri et al., 2000], which together accounts as much of the variation present in the original dataset and can be used to simplify the analysis and visualization of multidimensional data sets. PCs are eigenvectors of either the correlation or the covariance matrix, and variation associated with each PC is quantified by characteristics roots of the matrix, popularly called as eigenvalues. The variation explained by any PC is presented in the terms of its contribution to the all PCs, i.e. the eigenvalue of the selected PC divided by the sum of all the eigenvalues. PCs are mutually uncorrelated, orthogonal, linearly independent combination of the original variables. The first PC is a linear function of the variables and has maximum variance. The second PC is a linear function of the variables and orthogonal to the first PC with maximum variance. For a two variables example, an x-y graph could be plotted. A linear equation of x could be written in terms of y and vice versa, but these two equations are different as they are involved in reducing the points to line distance in either the x- or the y-direction but not both, and assume one independent

and one dependent variable [Fitzpatrick C., Ph.D. dissertation]. The first PC defines a best-fit line to the points, which reduces the perpendicular distance from the points to the line while the second PC is an orthogonal line to the first (Figure 2.11). The first PC captures the most variation followed by second. Similar theory is evolved for multiple variables case and number of PCs is equal to the number of variables, but each PC is orthogonal to the previous PC and responsible for less variation than the previous one. Also, better the correlations among variables, variability captured by first few PCs is most. It is important to note that PCA only gives useful results if number of PCs are significantly fewer than the number of variables responsible for most variation. The sign of a PC coefficient is usually arbitrary but the sign of a PC coefficient relative to the signs of other PCs coefficient is important to evaluate the variability. PC coefficients with same sign, relate to the variability that the variables have in common while different signs relate to the differences in the variability. Also, if a PC has nearly equal coefficients with same sign then the PC is a weighted average of all variables. An increase or decrease in one variable will affects all variables equal increase or decrease, respectively. In anatomic terms, PCs with coefficients of the same sign describe size variation in the specimen, as all dimensions are varying in the same direction; PCs with coefficients of different signs describe shape variation in the specimen. It often happens that the characteristic roots associated with the last few PCs are small and of similar magnitude. If characteristic roots are equal, or nearly equal, their PC axes will be almost equal in length, and have similar variances. The orientation of the PC axes depends on the axes of maximum variance. If variances are similar, the axes can be anywhere as

long as they are orthogonal, hence the orientation of the axes are not defined with much precision and interpretation of these PCs may be uninformative or misleading.

PCA has been used in a wide range of biomedical problems and has been shown to effectively create statistical shape models without significant loss of information from original data. PCA operates on the registered data of the training set, develops a statistical shape model which defines modes of variation and by perturbing these modes by some standard deviation, new instances can be created.

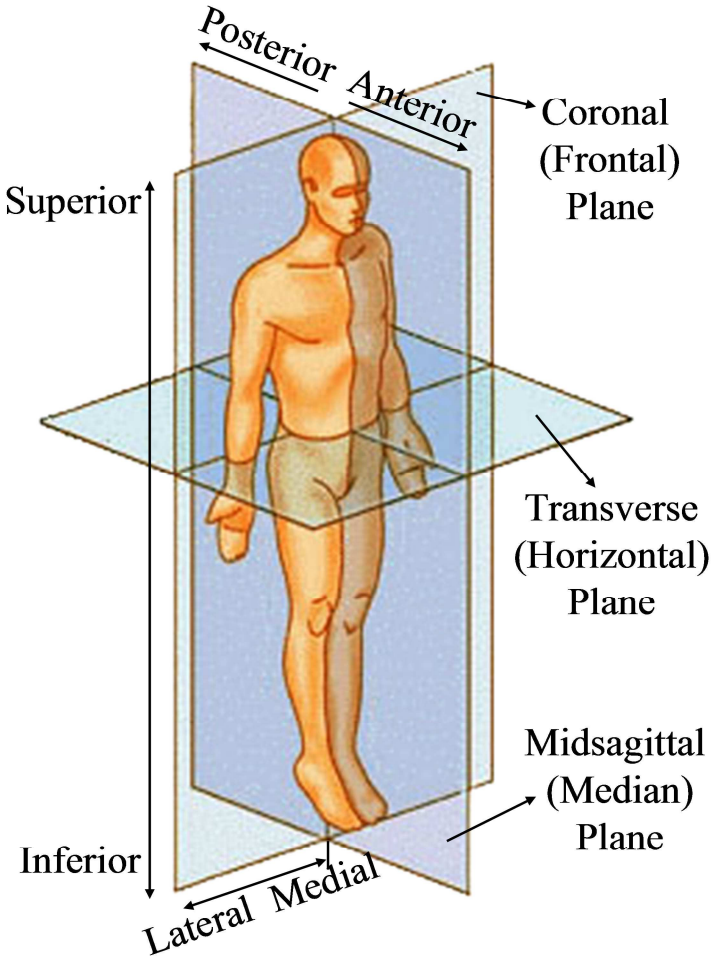

Figure 2.1: Clinical terms for anatomical planes and description of relative position (SEER's Training Website, 2004).

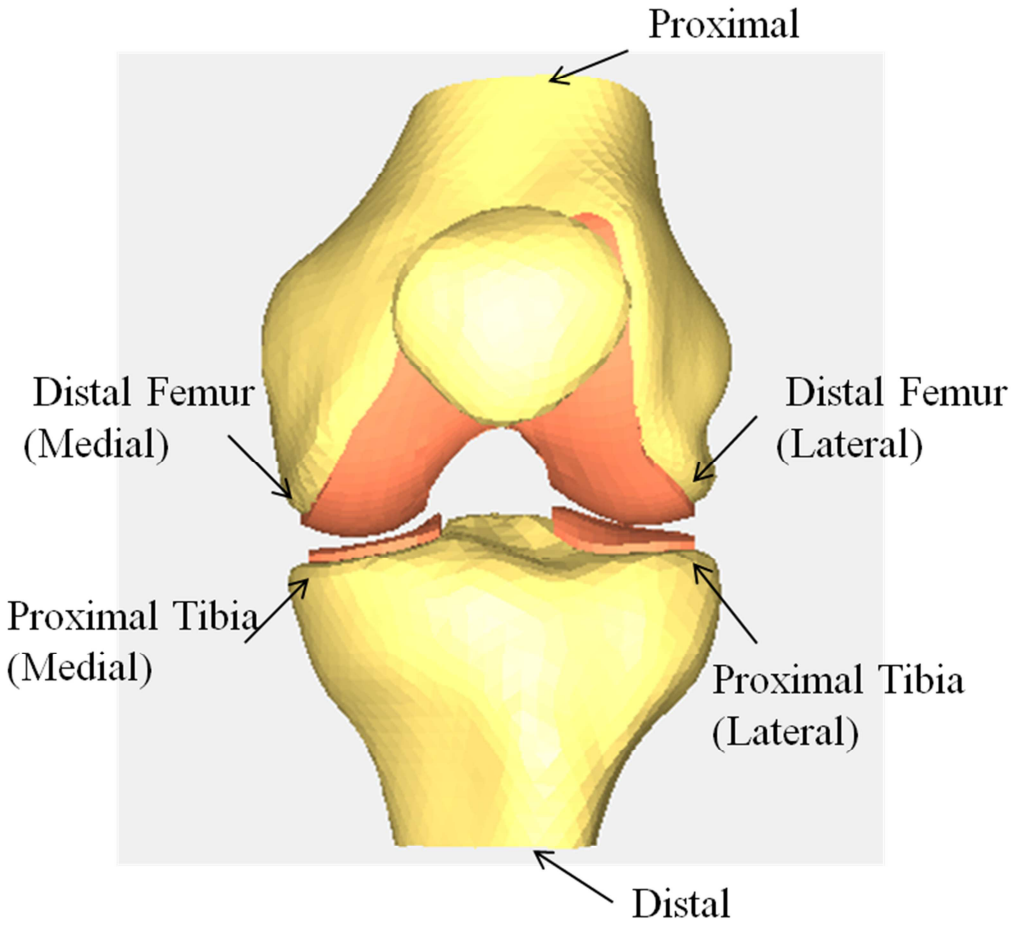

Figure 2.2: Clinical terms, proximal and distal to indicate an object proximity to the center of the body.

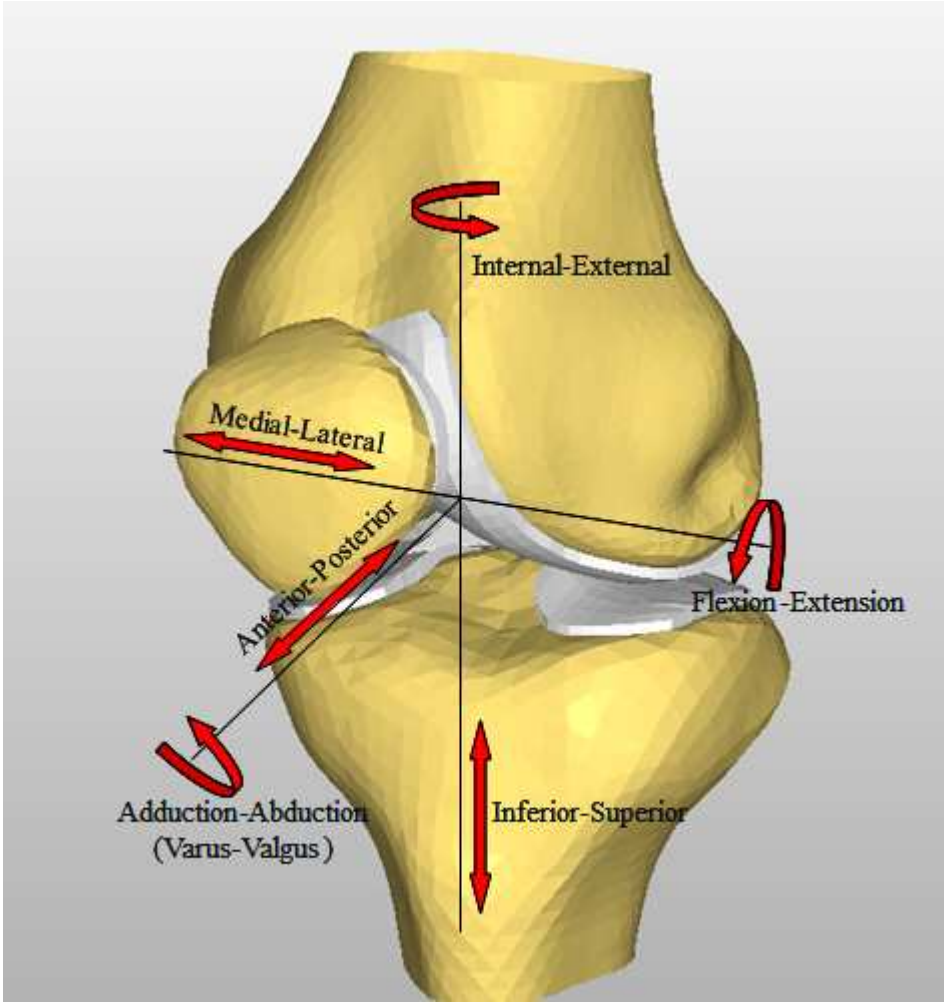

Figure 2.3: Kinematics terminologies to describe the six degrees of freedom (DOF) of the knee joint. Three of the DOF are translations along the anterior-posterior, medial-lateral, and inferior-superior axes defined at the joint, whereas the other three DOF are rotations around the each axis.

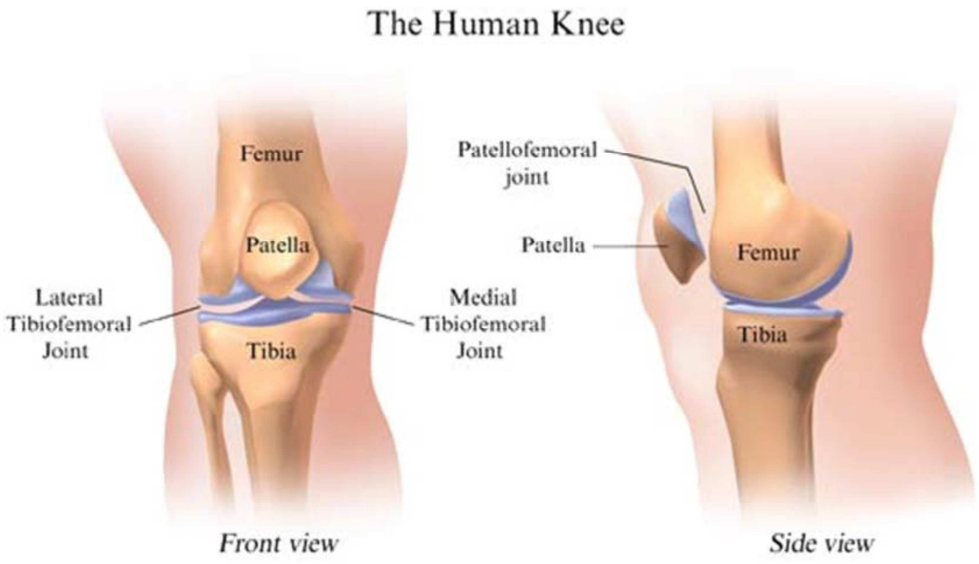

Figure 2.4: Diagram of bones and joints of the natural knee (www.mayclinic.org).

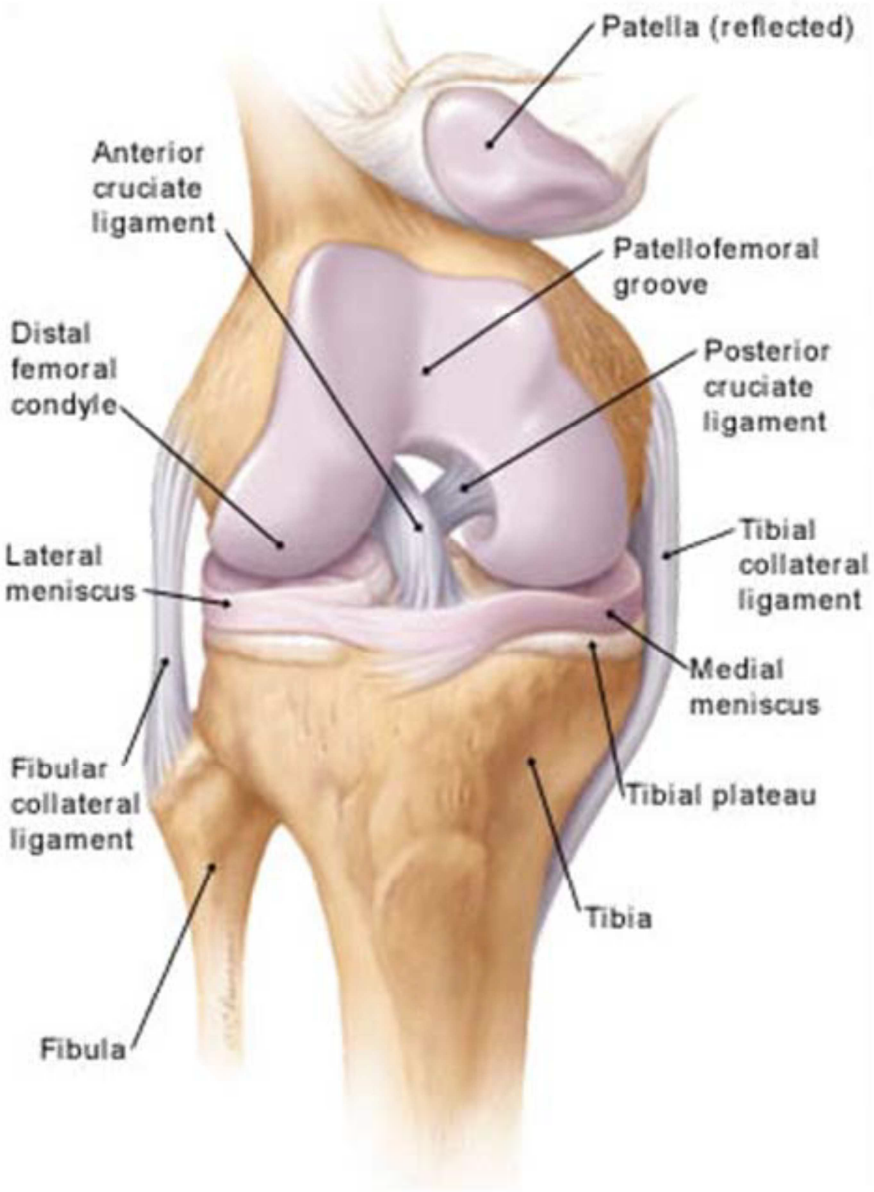

Figure 2.5: Diagram representing the soft tissue structures crossing the tibiofemoral joint of the knee (www.larsligament.com).

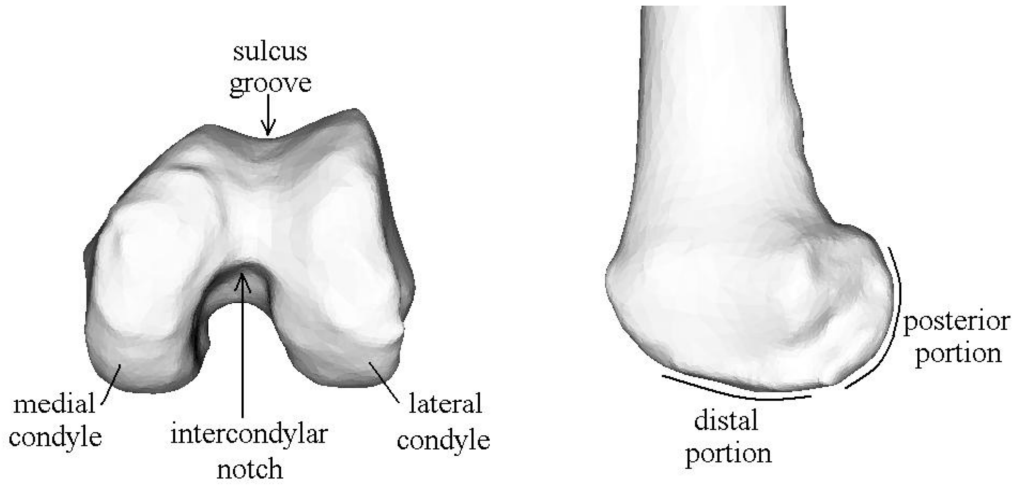

Figure 2.6: Femoral geometry: Left image shows the medial and lateral condyle, sulcus groove and intercondylar notch, viewed superiorly in the axial plane; Right image shows the distal and posterior segments of the lateral condyle, viewed laterally in the sagittal plane. (Source: Ph.D. dissertation, Fitzpatrick C.).

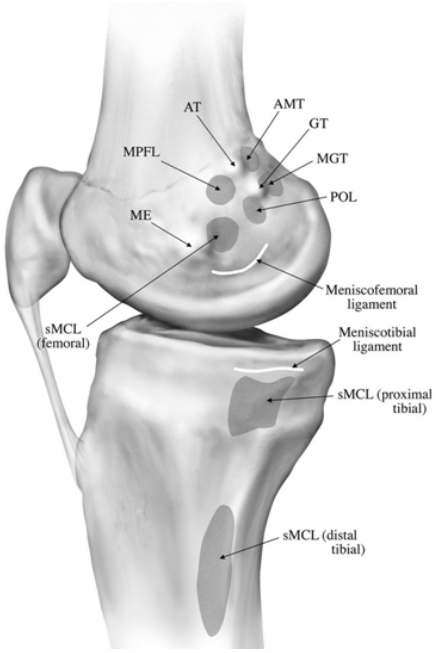

Figure 2.7: Illustration of the sMCL (superficial medial collateral ligament) attachment sites at femoral, proximal tibial and distal tibial (Laparde et al., 2007).

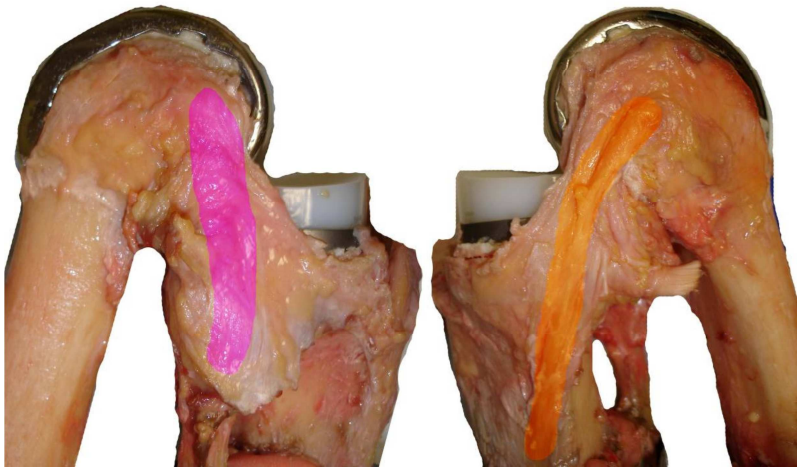

Figure 2.8: The location of the medial collateral ligament (orange) and lateral collateral ligament (purple) in deep knee flexion (Source: Ph.d. Dissertation, Chadd Clary).

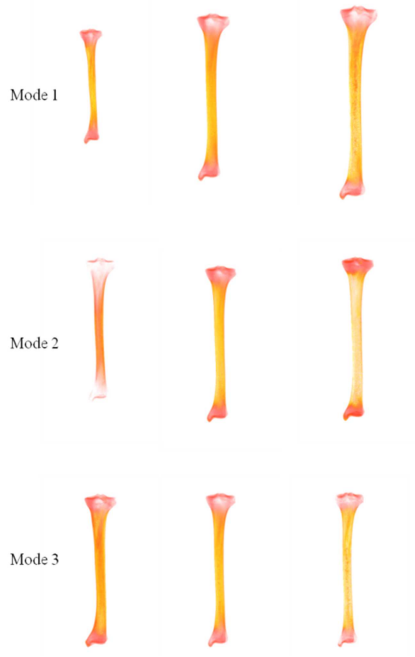

Figure 2.9: Tibia shapes of the first 3 PCs in isolation. Top to bottom are modes 1 to 3, left to right are PC weights sampled at −3 std dev, 0 std dev, and +3 std dev (Source: Ph.d. Dissertation, Francis Galloway).

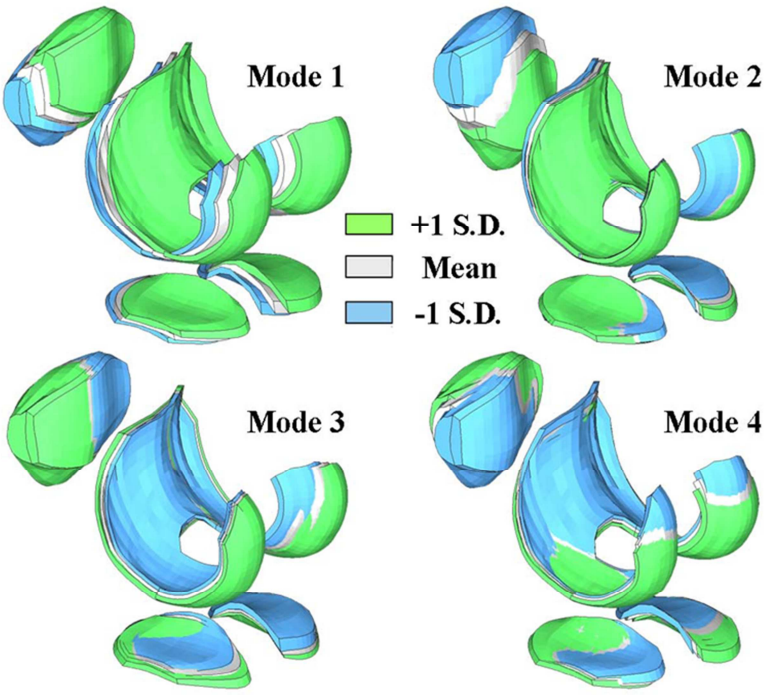

Figure 2.10: Statistical shape model of the knee showing mean and ±1 std dev geometries for the first 4 modes of variation (Baldwin et al., 2010).

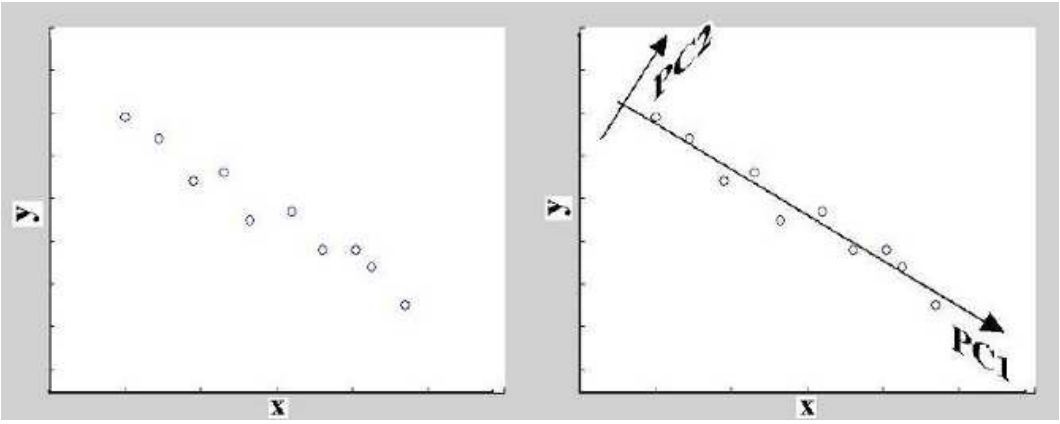

Figure 2.11: Left: Two variables, independent x and dependent y. Right: PC1 axis lies along the axis of maximum variation, with PC2 orthogonal to PC1, lying along the axis of maximum variation (Source: Ph.D. dissertation, Fitzpatrick C.).

CHAPTER 3 – METHODS

3.1 Training Set Preparation

The training set taken for statistical shape model (SSM) consists of MR image of 20 cadaveric specimens (Figure 3.1) and simulator test data. The specimens were all male with an average age of 66 years, average weight of 77 kg and average body mass index (BMI) of 25. The statistics of the specimens have been shown in Table 3.2. The training set data of this study basically contains shape and relative alignment data in terms of nodal co-ordinates and transformation matrix, respectively. Anatomical structures were constructed from MR image and their shape was represented by nodes linked to finite element meshes, while relative alignment between structures was obtained from simulator test data. Iterative closet point (ICP) was used to establish nodal correspondence of training set data and transformation matrices was used to characterize the relative alignment between the structures. This way, each member of the training set was represented by an equal number of data point.

3.1.1 Knee Construction

The structures of the 20 cadaveric knees (Figure 3.2), including femur, tibia, patella, associated cartilage and major ligaments (MCL, LCL, PCL, and ACL), were segmented from MR images with an in-plane resolution of 0.35 mm and an axial slice thickness of 1 mm, using ScanIP (Simpleware, Exeter, UK). As the scanned field of view varied between specimens in the training set, the femur and tibia were transected based on a constant aspect ratio between the medial-lateral width and the inferior-superior length. The details of the measurements and transected length of femurs and tibias have been shown in Table 3.3 and Table 3.4, respectively.

3.1.2 Registration for Correspondence

A template mesh for each bony structure was developed for an average member of the training set using tetrahedral elements (Figure 3.3). An iterative closest point (ICP) algorithm was utilized to register the training set geometries to the template mesh. To facilitate registration, the subject meshes were considerably finer than the template mesh; average edge lengths were 0.4 mm for the femur and tibia and 0.15 mm for the patella compare to 3.0 mm for the template. In the ICP algorithm, the nearest neighbor searching was accelerated using k-dimensional (k-d) trees similar to [Bryan et al., 2010] and distance along the normal of an element was used over Euclidean distance for structures with high curvature (femoral condyle). In this process each bone was registered to each other with nodal correspondence (Figure 3.4).

The cartilage structures were represented by hexahedral (hex) meshes because of their improved behavior in finite element analyses with contact. Each cartilage was segmented and aligned with the associated bone. Nodal handles were used to volume-morph the hexahedral mesh template to the subject-specific model using custom TCL/VTK script and Hypermorph (Altair, Troy, MI)[Fitzpatrick et al., 2012]. The script generated 1200, 264, 240 and 390 handles for femoral-cartilage, tibial-medial-cartilage, tibial-lateral-cartilage, and patellar-cartilage geometries, respectively, and produced three layers of hexahedral elements (2748, 990, 825, and 504 elements for each cartilage, respectively) across the thickness of each cartilage.

3.1.3 Relative Alignment and Transformation Vector

MR scans are typically performed in full extension without an applied load on the quadriceps or a known flexion angle. If alignment of the structures was based on this uncontrolled, unloaded position, it is difficult to determine whether the variability observed is due to relative alignment of the structures or differences in scan position.

Based on the as-scanned position, knee flexion varied from -2° to 18°. As an alternative to reporting alignment based on this uncontrolled and unloaded position, the structures of the knee were aligned to a known position in the Kansas knee simulator with the quadriceps loaded to maintain a tibiofemoral flexion angle of 30°. The process aligned each meshed structure to kinematic data collected during the experiment and test probed point data for each structures (Figure 3.5).

Local anatomic coordinate systems were developed for each bone based on the articular geometry and anatomical landmarks [Pandy et al., 1997; Morton et al., 2008] *(Appendix A).* The femoral coordinate system was defined with the origin at the center of the axis of the cylinder fit through the medial and lateral condyles of the femur [Pandy et al., 1997; Della et al., 1999], medial and lateral epicondylar points and the line passing through the centroids of three slices at the proximal end of the femur [Morton et al., 2008]. The tibial coordinate system was constructed with the origin at the medial tibial eminence, using lines passing through centroids of three slices at the distal end, and through the centers of the tibial condyles [Morton et al., 2008]. The patellar coordinate system was developed using the proximal, distal, and lateral points around the articular periphery with the origin located at the geometrical centroid [Morton et al., 2008; Armstrong et al., 2003]. The kinematic alignment of the tibial and patellar coordinate systems relative to the femoral coordinate system was represented by 4x4 transformation matrices. A transformation matrix is a tool for simplification of coordinate transformations and it includes information about translations and rotations. A typical 4x4 transformation matrix (TF) has been shown in equation 3.1.

$$TF = \begin{bmatrix} R_{xx} & R_{xy} & R_{xz} & P_x \\ R_{yx} & R_{yy} & R_{yz} & P_y \\ R_{zx} & R_{zy} & R_{zz} & P_z \\ 0 & 0 & 0 & 1 \end{bmatrix} \qquad \text{Equation 3.1}$$

The position vector P represents the translation from the global to the local coordinate systems and the rotation sub-matrix R denotes the rotations of each axis in body 1 about body 2. Note that the rotation sub- matrix is a multiplication matrix of the dot products of the unit vectors of the two body coordinate systems; therefore each column of R indicates the orientation of the local axis with respect to the corresponding global axis.

During the process of alignment of constructed structures to the probed points and the development of relative transformation matrix, a series of steps were followed. The cartilage probed point test data were reported in their respective rigid body frame. As each rigid body reference frame transformation (4x4) was given with respect to the global origin (camera origin), tibial and patellar cartilage probed points were transformed to the femoral rigid body space for an unknown flexion angle. Next, the constructed geometries from their local coordinate space were aligned to their respective probed points and during this process their coordinate systems were also moved along. In this way, local anatomical axes of each bone was made available for the further transformation and structures were aligned to the 30^0 known flexion position with femoral origin as global origin. Further, relative transformation of tibia and patella to the femur was developed in the form of 4x4 transformation matrix (Equation 3.1).

3.2 Principal Component Analysis

The variability in shape and alignment was characterized by performing a principal component analysis (PCA) on the training set data. PCA is a statistical technique to decompose a large data set into its significant principal components in terms of eigenvalues and eigenvectors.

3.2.1 Bones Only

In the bones only case, SSAM was developed by PCA on the following data: x,y,z coordinates defining the knee structures (2384, 1101 and 472 nodes for the femur, tibia and patella, respectively) reported in their local anatomical coordinate system and 24 terms of the transformation matrix relating the position of the tibia and patella to the femur (4x4 transformation: 3x3 rotations and 3 translations for each tibiofemoral and patellofemoral joint). Matrix size for the PCA was 11895x20 and contains:

-x,y,z coordinates defining the nodes for the knee bones: femur, patella, and tibia reported in their local anatomical coordinate system

-Components of the transformation matrix relating the position of the tibia and patella to the femur (4x4 transformations)

PCA was performed on the covariance matrix after the mean was subtracted from the original data

3.2.2 Bones and Cartilages

In this case, bones cartilages: femoral, tibial-medial, tibial-lateral and patellar cartilages were added to bones. In addition to 11895 terms for each member in the training set, 6282 terms were added for the cartilages. Hence, each member of the training set is represented by the following data points:

-x,y,z coordinates defining the nodes and morphing handles for the knee structures reported in their local anatomical coordinate system

-Components of the transformation matrix relating the position of the tibia and patella to the femur (4x4 transformations)

For reference, the template mesh for the femur, tibia and patella consisted of 2384, 1101 and 472 nodes, respectively. The cartilage structures were represented by 2094 nodes, which served as morphing handles for a finer mesh. The alignment transformations included 24 terms, defining 3x3 rotations and 3 translations for the tibiofemoral and patellofemoral transformations. PCA was performed on the covariance matrix after the mean was subtracted from the original data. As a result, a series of modes of variation-some corresponding to size and shape, others were corresponding to relative alignment of the structures.

The most common changes in shape and alignment can be visualized by perturbing specific modes of variation based on their corresponding eigenvalues and eigenvectors.

3.2.3 Bones and Cartilages and Ligament Attachments Site

After demonstrating SSAM generation for bones and cartilages successfully, four major ligaments (MCL, LCL, PCL, and ACL) attachment points were added for the training set. MCL was represented by 3 attachment sites: medial femoral epicondylar point, medial proximal tibia and medial distal tibia while LCL was represented by two attachment sites: lateral femoral epicondylar point and fibula proximal end (Figure 3.6). Cruciate attachment areas were taken as antero-medial (amACL) and postero-lateral (plACL) for the ACL and postero-medial (pmPCL) and antero-lateral (alPCL) for the PCL (Harner et al., 1999) (Figure 3.7). Femoral and tibial cruciate attachment areas were approximately quartered *(Appendix B)* to place four attachment points at the centroid of each quadrant while each collateral ligament site was represented by a point. All considered ligament attachment points have been shown for mean specimen of training set specimen in Figure 3.8.

Inclusion of the ligaments attachments sites added 10 nodes on the femur and 11 nodes on the tibia, resulting 63 more rows (x,y,z for each nodes) to each member of training set and making the matrix size as 18240x20. PCA was performed in the same way as described above.

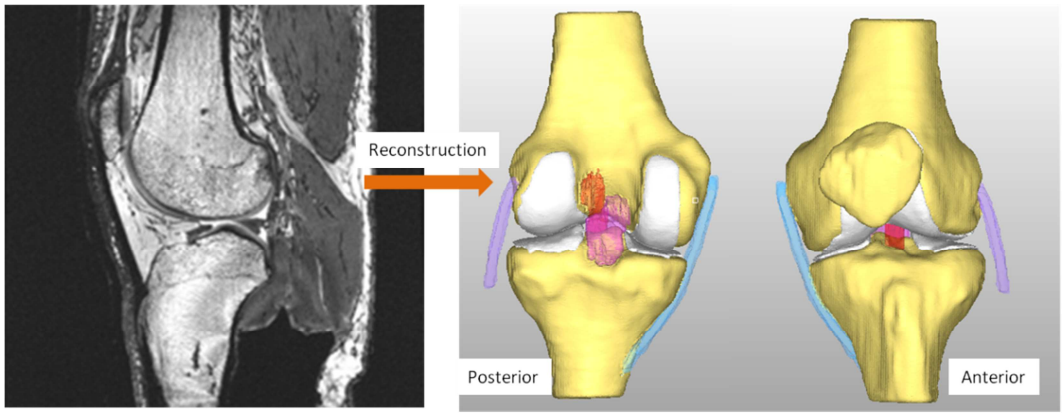

Figure 3.1: Knee structures reconstruction from stacks of 2-dimensional MR images (left image) in the form of 3-dimensional StereoLithography (.stl) format (right image).

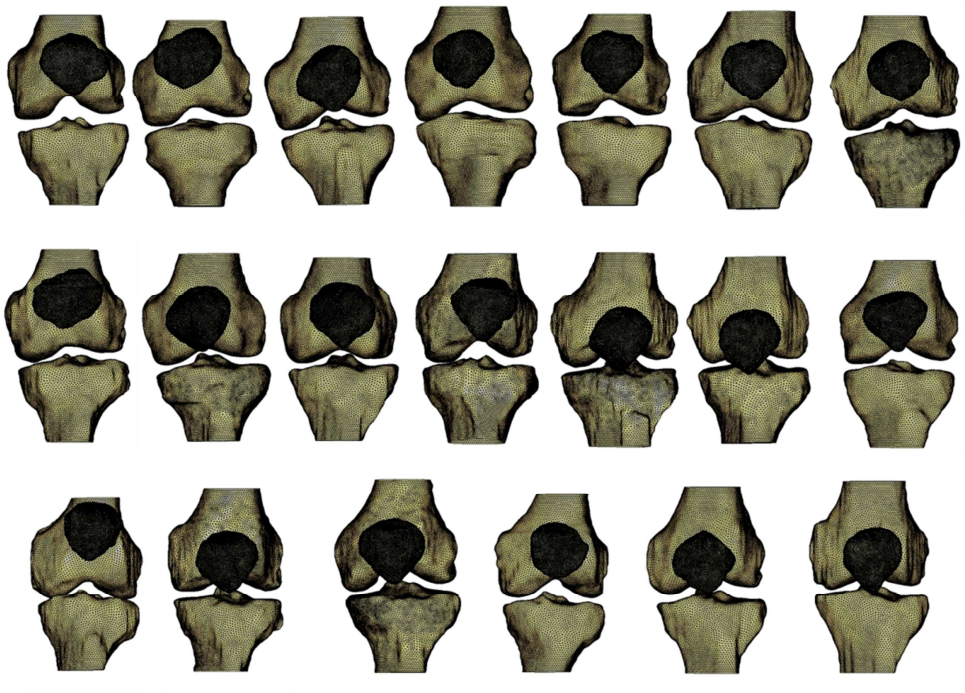

Figure 3.2: Reconstructed and processed bones of 20 specimens of the training set in scan space and illustrating the shape and size variability among them.

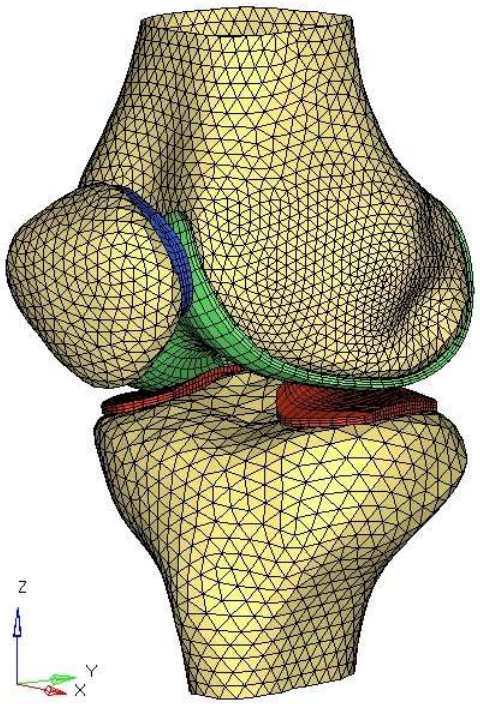

Figure 3.3: An average template mesh with 3.0 mm element edge length, used for establishing nodal correspondence through ICP, between training set.

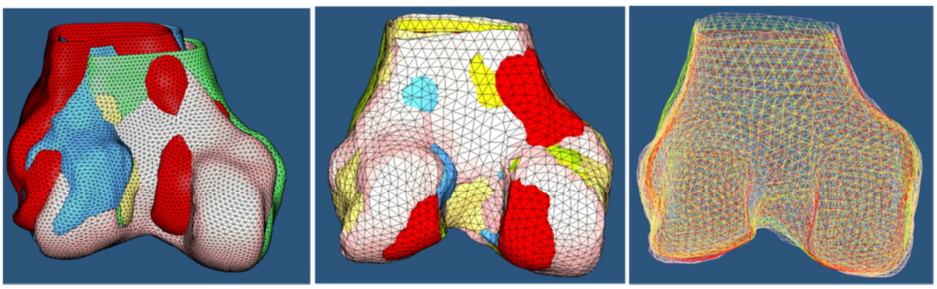

Figure 3.4: Left- Unregistered femurs before ICP registration technique, Middle- shell representation of registered femurs to the template femur for establishing nodal correspondence and each femur has equal number of nodes, Right- Wireframe representation of registered femurs.

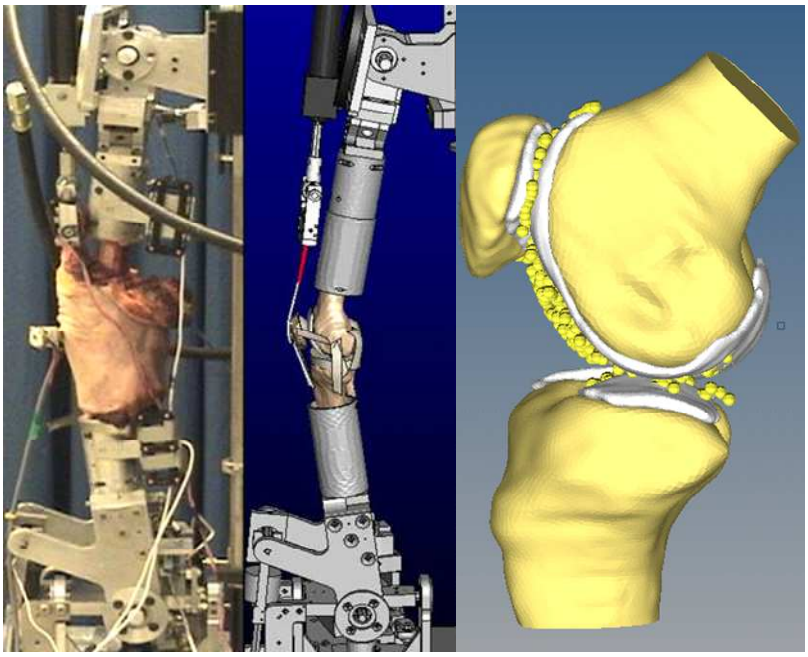

Figure 3.5: Left- A cadaveric specimen is being tested for an activity in the Kansas Knee Simulator, Middle-Computational model representation of knee simulator with a virtual knee model, Right- Reconstructed knee aligned to cartilage probed points corresponding to 30 degree flexion, obtained during knee simulator test.

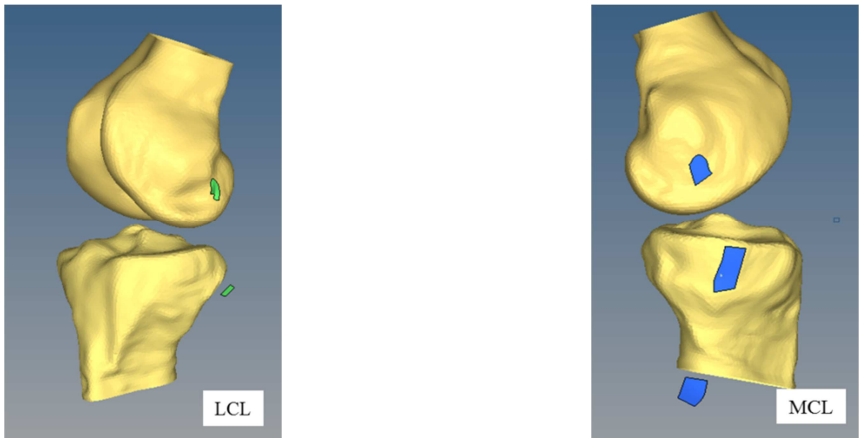

Figure 3.6: Constructed collateral ligament attachment sites surface geometry from one of the subject in the training set; Left- lateral collateral ligament represented by lateral femoral epicondylar site and fibula proximal end site, Right- medial collateral ligaments represented by medial femoral epicondylar, medial proximal tibia and medial distal tibia site.

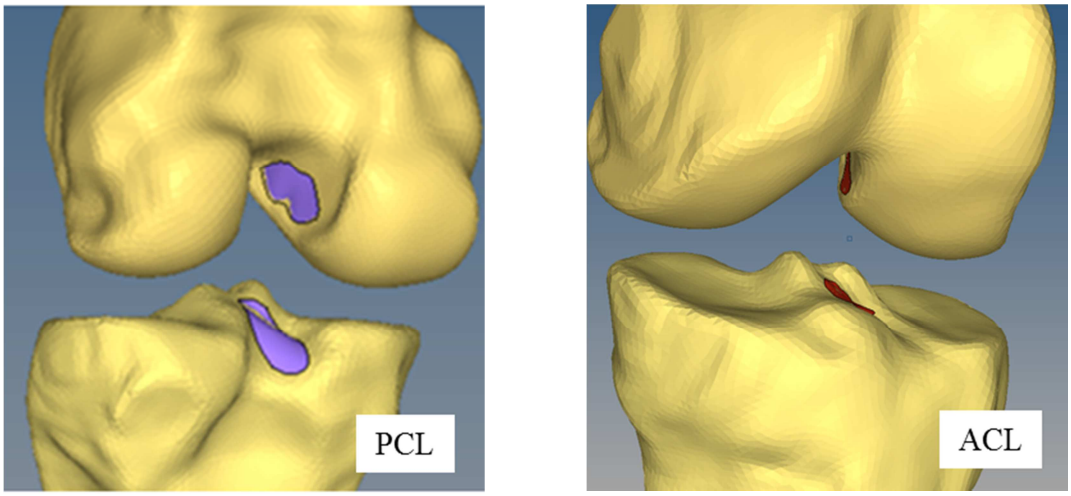

Figure 3.7: Constructed cruciate ligament attachment sites surface geometry from one of the subject in the training set; Left- posterior cruciate ligament attachment site on femur and tibia, Right- anterior cruciate ligament attachment site on femur and tibia.

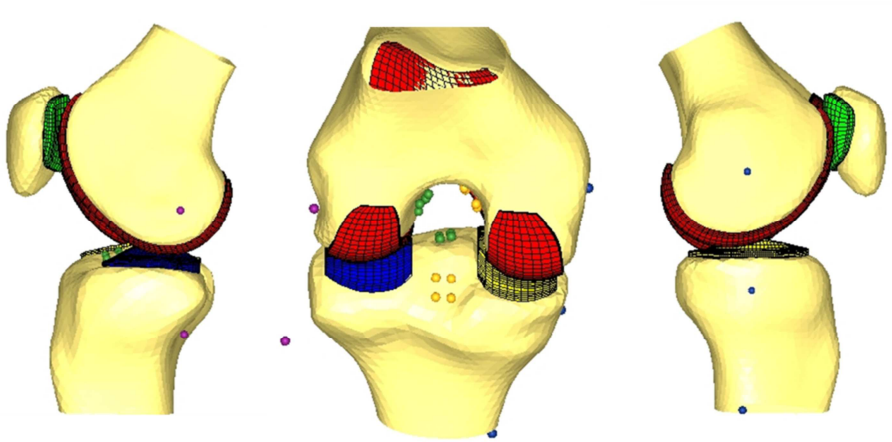

Figure 3.8: Ligament attachment sites for the mean subject of the training set; Left- lateral collateral ligaments represented by lateral femoral epicondylar point and fibula proximal end, Middle- femoral and tibial cruciate attachment areas were quartered to place four attachment sites at the centroid of each quadrant, Right- medial collateral ligaments represented by medial femoral epicondylar point, medial proximal tibia and medial distal tibia.

Table 3.1: Demographic details of specimens used in study.

Subjects	Sex	Age (years)	Height (m)	Height (in)	Weight (kg)	Weight (lbs)	BMI
BB02	M	80	1.83	72	92.98	205	27.80
BB03	M	55	1.68	66	81.64	180	29.05
BB04	M	59	1.78	70	63.50	140	20.09
BB06	M	59	1.78	70	63.50	140	20.09
BB07	M	80	1.83	72	92.98	205	27.80
BB08	M	61	1.83	72	90.72	200	27.12
BB09	M	80	1.83	72	92.98	205	27.80
BB11	M	55	1.68	66	81.64	180	29.05
BB12	M	59	1.78	70	63.50	140	20.09
BB14	M	68	1.83	72	100.00	220	29.90
BB16	M	72	1.66	65	68.18	150	24.95
BB17	M	63	1.85	73	77.11	170	22.45
BB24	M	74	1.75	69	81.65	180	26.66
BB25	M	60	1.75	69	60.78	134	19.79
BB26	M	52	1.73	68	72.58	160	24.33
BB27	M	79	1.73	68	74.39	164	24.94
BB29	M	77	1.73	68	86.18	190	28.89
BB30	M	52	1.73	68	72.58	160	24.33
BB32	M	64	1.75	69	61.24	135	19.94
BB34	M	71	1.78	70	70.31	155	22.24

Table 3.2: Statistics of specimens used in study.

	Age (years)	Weight (kg)	BMI (kg/m^2)
Mean	66	77.42	24.86
Standard	9.90	12.26	3.57
Max	80	100.00	29.90
Min	55	60.78	19.79

Table 3.3: The details of the truncated femur length to achieve same aspect ratio (BB27 was the reference) for the training set subjects.

Subjects	ML width (mm)	SI length (mm)	Width/Length (Ratio)	New SI length (Length/ Max. Ratio)	Truncated SI length (mm)
BB02	82.96	94.56	0.88	74.36	20.20
BB03	84.098	100.404	0.84	75.38	25.03
BB04	88.91	105.66	0.84	79.69	25.97
BB05	78.76	101.58	0.78	70.59	30.99
BB06	91.906	100.866	0.91	82.38	18.49
BB07	81.122	94.772	0.86	72.71	22.06
BB08	88.327	95.327	0.93	79.17	16.16
BB09	90.62	104.21	0.87	81.22	22.99
BB11	87.7	101.13	0.87	78.61	22.52
BB12	87.42	105.22	0.83	78.36	26.86
BB13	87.62	103.13	0.85	78.53	24.60
BB14	83.97	101.17	0.83	75.26	25.91
BB16	86.95	93.23	0.93	77.93	15.30
BB17	90.72	89.36	1.02	81.31	8.05
BB18	80.8	89.15	0.91	72.42	16.73
BB19	90.383	94.617	0.96	81.01	13.61
BB20	82.992	87.461	0.95	74.39	13.07
BB24	84.331	85.007	0.99	75.59	9.42
BB25	84.635	90.061	0.94	75.86	14.20
BB26	80.54	84.58	0.95	72.19	12.39
BB27	81.78	73.3	1.12	73.30	0.00
BB29	88.94	99.6	0.89	79.72	19.88
BB30	82.2	90.3	0.91	73.68	16.62
BB31	88.816	90.877	0.98	79.61	11.27
BB32	84.364	88.624	0.95	75.62	13.01
BB34	86.17	85.167	1.01	77.23	7.93

Table 3.4: The details of the truncated tibia length to achieve same aspect ratio (BB16 was the reference) for the training set subjects.

Subjects	ML width (mm)	SI length (mm)	Width/Length (Ratio)	New SI length (Length/ Max. Ratio)	Truncated SI length (mm)
BB02	78.65	79.73	0.99	62.76	16.97
BB03	78.782	83.736	0.94	62.86	20.87
BB04	79.7	77.07	1.03	63.59	13.48
BB05	74.75	84.12	0.89	59.64	24.48
BB06	85.234	85.187	1.00	68.01	17.18
BB07	79.733	83.293	0.96	63.62	19.67
BB08	84.24	89.765	0.94	67.22	22.55
BB09	81.71	82.6	0.99	65.20	17.40
BB11	79.6	83.04	0.96	63.51	19.53
BB12	79.52	81.44	0.98	63.45	17.99
BB13	79.35	83.7	0.95	63.32	20.38
BB14	78.59	85.46	0.92	62.71	22.75
BB16	79.03	63.06	1.25	63.06	0.00
BB17	80.55	67.52	1.19	64.27	3.25
BB18	72.97	65.4	1.12	58.22	7.18
BB19	83.744	69.955	1.20	66.82	3.13
BB20	75.581	67.678	1.12	60.31	7.37
BB24	79.466	80.321	0.99	63.41	16.91
BB25	72.67	59.53	1.22	57.98	1.55
BB26	72.68	72.4	1.00	57.99	14.41
BB27	76.29	70.6	1.08	60.87	9.73
BB29	82.89	80.5	1.03	66.14	14.36
BB30	72.66	63.92	1.14	57.98	5.94
BB31	81.731	86.667	0.94	65.22	21.45
BB32	78.224	75.801	1.03	62.42	13.38
BB34	80.889	69.079	1.17	64.54	4.54

CHAPTER 4 – RESULTS

4.1 Shape and Size and Alignment Variability

The findings of the current study are dually in the methodology to develop and the creation of the statistical shape and alignment model. The SSAM model described the variability in the training set with a series of modes of variation defined by eigenvalues and eigenvectors. By applying PCA, the data representing the variability in the training set is essentially reduced from the 18240 individual variables (nodal coordinates and transformations) to a series of nominally a dozen orthogonal variables. Each orthogonal variable represents a mode of variation described by an eigenvalue related to how much variability is explained by the mode and an associated eigenvalue depicting how each original variable is transformed.

4.1.1 Bones Only

The SSAM of the knee characterized the common modes of variation with the first 3 modes representing 70% of the variability and 10 modes representing 95% (Table 4.1). Characterizing 49% of the variability, mode 1 corresponded primarily to scaling with changes in size of the structures and associated scaling of alignment, but also included tibial varus-valgus (VV) alignment (Figure 4.1). Mode 2 (13% of variability)

captured changes in patella inferior-superior (alta-baja) position and tibial anterior-posterior (AP) position, while Mode 3 (8%) described changes in femoral condylar and trochlear geometry, patellar shape and tibial VV alignment (Figure 4.2).

4.1.2 Bones and Cartilages

In the statistical shape and alignment model, the first 3 modes of variation explained 47% of the variability, with 10 and 15 modes capturing 84.8% and 95.6% respectively (Table 4.2). Individual modes of variation are perturbed to visualize the modes of variation. Mode 1 (20% of variability explained) described scaling of all of the structures of the joint and also included patellar alta-baja alignment relative to the femur (Figure 4.3). Mode 2 (16%) described tibial anterior-posterior (AP) alignment and associated patellar alta-baja alignment, and the shape and internal-external (IE) alignment of the articular surfaces in the patella femoral joint (Figure 4.3). Mode 3 (11%) characterized tibial IE rotation and patellar shape, specifically the medial-lateral facet ratio (Figure 4.4). Mode 4 (8%) described tibial varus-valgus alignment and patellar alta-baja (Figure 4.4). Mode 5 (7%) captured subtler shape change in multiples structures, including medial-lateral width of the femoral and tibial cartilage (Figure 4.5).

4.1.3 Bones and Cartilages and Ligaments Attachment Sites

Addition of ligaments attachment sites point data set only added only 63 new rows (21 points x 3 coordinates) to bones plus cartilages data set. Hence, results were very much similar to previous case. So, in this case of statistical shape and alignment

modeling the first 3 modes (Table 4.3) of variation explained 47% of the variability with 10 and 15 modes captured 84.6% and 95.5%, respectively.

Mode 1 represented 20.6% of the variability and accounted for primarily scaling driven change in the size of the structures. As in, scaling of alignment with patella alta-baja and medial-lateral position variability were captured (Figure 4.5).

Mode 2 (16 % of variability) captured changes in tibial anterior-posterior alignment, shape; internal-external alignment of the patellofemoral joint; and femoral articular surface and depth of sulcus geometry (Figure 4.6).

Mode 3 (Figure 4.7) captured 11% of the variability and characterized tibial IE rotation and patellar shape, specifically the medial-lateral facet ratio.

4.1.4 Leave One Out Analysis

Leave one out analysis was performed on the bone plus cartilage training set data. This analysis evaluates the predictive capability [Ph.D. Dissertation, Galloway F., 2012] of the SSAM. During the analysis each knee was left out in turn and a SSAM was created using the remaining training set data. In this process, for each leave out case important PC vectors were calculated. These PC vectors and adjusted mean of variable of original (without left out) training set data were used to reconstruct the left-out knee. This was done for increasing number of the PCs, and each time the left out knee was estimated. As per the reconstruction test, the vertex position error was then computed between the ‘left-out’ tibia and ’estimated’ tibia. The mean Euclidean distance error and inter-quartile range between model predicted and actual geometries is reported as a box plot (Figure 4.8) showing that the errors reduce with an increasing number of the modes

of variation included. The distribution represented in the box plot characterizes the variability in the analysis leaving out each member of the training set. The results converge when more than 12 modes are included in the model prediction. Using the first 15 modes of variation (which characterized 95% of the variability), the average mean error was 1.64 mm with a standard deviation of 0.21.

4.2. Fidelity of Statistical Shape Models

Finite element analyses were performed on models generated from the statistical shape and alignment. Joint mechanics were evaluated for the average and first 2 modes at +/- 1 standard deviation.

4.2.1 Finite Element Analysis

Further, the link to joint mechanics prediction is demonstrated by evaluating the contact mechanics with finite element analyses for a series of virtual subjects: mean and modes 1 and 2 evaluated at ± 1 standard deviation. The model geometry and alignment was derived from the statistical shape and alignment model. The extensor mechanism, based on [Baldwin et al., 2009] and [Fitzpatrick et al., 2011] was morphed to the new geometry. In the analysis, the tibia was fixed with a load representative of body weight (660N) applied to the femur and a distributed 1000 N load applied through the extensor mechanism. Bones were modeled as rigid and cartilage was modeled as a fully deformable linear elastic material [Mesfar and Shirazi–Adl, 2005]. Contact pressure and area are shown at 30° tibiofemoral flexion (Figure 4.9).

4.3 Discussion

This study developed a methodical approach for statistical shape modeling of the knee joint. The statistical shape model characterized intersubject variability for a population of knees. The statistical model was developed with the shape of the knee described relative to the local anatomic coordinate system for each structure, while alignment between the structures of the joint was determined for controlled, known position.

The shape model included tibiofemoral (TF) and patellofemoral (PF) joints of the knee in the study. Knee joint structures: bones- femur, tibia, and patella; cartilages- femoral, tibial-medial, tibial-lateral, and patellar; ligaments- attachment sites of MCL, LCL, PCL, and ACL were used to represent each knee.

The structures of knee were segmented from MR images using ScanIP (Simpleware, Exeter, UK). The femur and tibia were transected based on a constant aspect ratio between the medial-lateral width and the inferior-superior length to normalize the intersubject bone length because of the variation in the scanned field of view. The images had an in-plane resolution of 0.35 mm (pixel size) and an axial slice thickness of 1 mm. The slice thickness and pixel size of a scan determine the accuracy of the reconstructed model. During the process of reconstruction the curvature of the bone is obtained by interpolating between the slices. Therefore, it is important to note that the interpolation may have caused some detail loss but the overall shape of the bone was maintained by visual inspection. Also, a relatively finer mesh (close comparison to the in-plane resolution of the scan) with average element length of 0.4 mm for femur and

tibia and 0.15 mm for patella were used for the registration to the template. However, analysis to measure out the repeatability of methods can be a quantifying tool for the segmentation error.

MR scans are typically performed in full extension without an applied load on the quadriceps and hence flexion angle varied from -2° to 18°. So, instead of scan position, loaded position from the knee simulator activity was used to capture the relative alignment between knee structures. The relative alignment between knee structures was based on the time point corresponding to the desired flexion during the simulator activity. In this approach, the time point varied across the subjects to achieve a fixed flexion. It is important to note that there can be variability in the load applied to the knee to achieve a fixed flexion position. Two instances of loaded position, i.e. 30^0 and 15^0 flexion, were used in the study.

The availability of simulator data limited the size of the training set to 20 specimens and an all-male population. The test probed points of the four cartilages (femoral, tibial-medial, tibial-lateral, and patellar) collected during the simulator activity were first aligned relative to each other using transformation matrices data collected during the experiment. Segmented geometries of each knee were discretized in the nodal form and the positioning was done to test probed points data for each structure for an unknown flexion. The test probed points collected for random locations during the experiment were not sufficient enough to perfectly position the structures. Therefore, using best judgment was the basis for positioning the structures to the probed points and, utilizing the reference axes of each bone and the activity data, the structures were rotated

to obtain a fixed flexion. Moreover, a slight positioning error of the structures to the probed points was carried over to the fixed flexion position during the rotation of the structures. The local coordinate systems were developed for the template subject using established procedures and subsequently transferred to each subject in the training set after performing the iterative closest point alignment. The iterative closet point alignment also registered training set subjects to the template subject for node-to-node correspondence. Local coordinate systems of each structure were preserved while positioning the registered model from template space to simulator space. The reported alignment was based out of positioned structures for fixed flexion in the simulator space. Notably, there is a greatest uncertainty associated with aligning the segmented geometry to experimentally-measured limited probed point cloud data. This could be a potential source of error.

Principal component analysis on the data consisting of shape and relative alignment yielded important modes captured together with all variability in the data. The shape and alignment model representing new virtual subjects was developed by perturbing the modes with +/2 std. dev. Important modes of variations were studied with additional structural complexities and for two known positions, i.e. 30^0 and 15^0 flexion.

Investigations of the modes yielded insight into the shape and alignment relationships between the structures. In the study involving bones, cartilages, ligament attachment sites, and 30^0 flexion, the first 3 modes of variation explained 47% of the variability with 10 and 15 modes capturing 84.6% and 95.5%, respectively. Mode 1 represented 20.6% variability, primarily scaling driven. Mode 2 (16% of variability)

captured changes in tibial anterior-posterior alignment, internal-external alignment of the patellofemoral joint, and femoral articular surface and depth of sulcus geometry. Mode 3 (11%) characterized tibial internal-external rotation and patellar shape, specifically the medial-lateral facet ratio.

Strong correlations are desirable in reducing the number of relevant modes. The strength of the PCA-based statistical modeling approach is its ability to capture and maintain these subtle geometric and alignment changes. In the present study when multiple structures of the knee were considered, the first few modes of variation (20.6%, 16% and 11% for modes 1, 2 and 3) explained less variability. Bryan et al. [2009] reported 45% of the variability was explained by mode 1 and more than 75% was captured with the first 8 modes in their study of the femur. When considering only the bones (femur, tibia and patella) and alignment in the current study, the first mode of variation explained 49% of the variability.

Leave one out analysis was performed and the results converged when more than 12 modes were included in the model prediction. For the first 15 modes of variation (which characterized 95% of the variability) the average mean error was 1.64 mm with a standard deviation of 0.21.

The fidelity of shape models was studied after performing finite element analyses for joint mechanic predictions. Joint mechanics were evaluated for the average and the first 2 modes at +/- 1 standard deviation. In the study, a fixed loading was applied to the models evaluated. However, it would be more realistic to scale the applied loading proportionate to specific anatomic measurements [Bryan et al., 2009].

This piece of study demonstrated the workflow for the development of the statistical shape modeling to characterize anatomical variability of the knee and generated new virtual subjects in finite element analysis format.

Table 4.1: Bone Only: Cumulative variability explained and description of characterized behavior for the most significant modes of variation.

Mode	Variability explained (Percent)	Mode characteristics
1	49	Scaling with changes in size of the structures and associated scaling of alignment, but also included tibial varus-valgus (VV) alignment
2	13	Patella inferior-superior (alta-baja) position and tibial anterior-posterior (AP) position
3	8	Changes in femoral condylar and trochlear geometry, patellar shape and tibial VV alignment

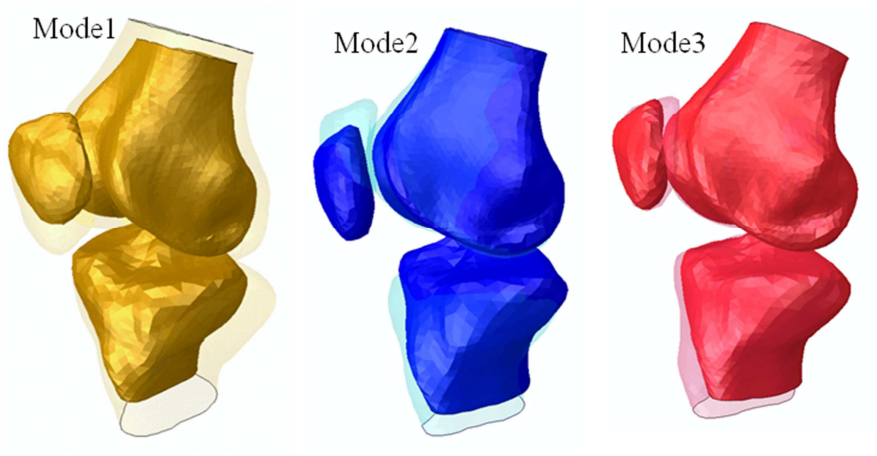

Figure 4.1: Modes of variation for the statistical shape and alignment model shown at +/- 2 standard deviations. Mode 1 capturing scaling in size and tibiofemoral VV alignment.

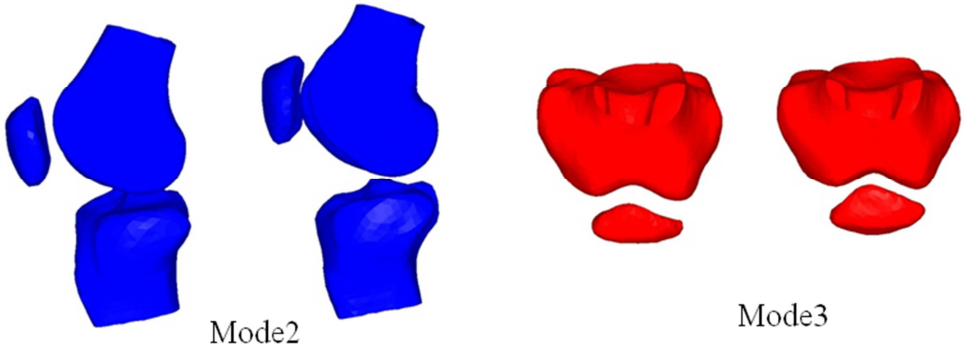

Figure 4.2: Mode 2 relation between tibial AP position and patella alta-baja. Mode 3 relation in shape for the trochlear groove and patella .

Table 4.2: Bone Plus Cartilages: Cumulative variability explained and description of characterized behavior for the most significant modes of variation.

Mode	Cumulative variability explained (Percent)	Mode characteristics
1	20.2	Scaling, patellar alta-baja
2	36.1	Tibial anterior-posterior alignment, shape and internal-external alignment of the patellofemoral joint
3	47.5	Tibial internal-external rotation, patellar shape (medial-lateral facet ratio)
4	55.5	Tibial varus-valgus and patellar alta-baja
5	62.6	Medial-lateral width of femoral and tibial cartilage

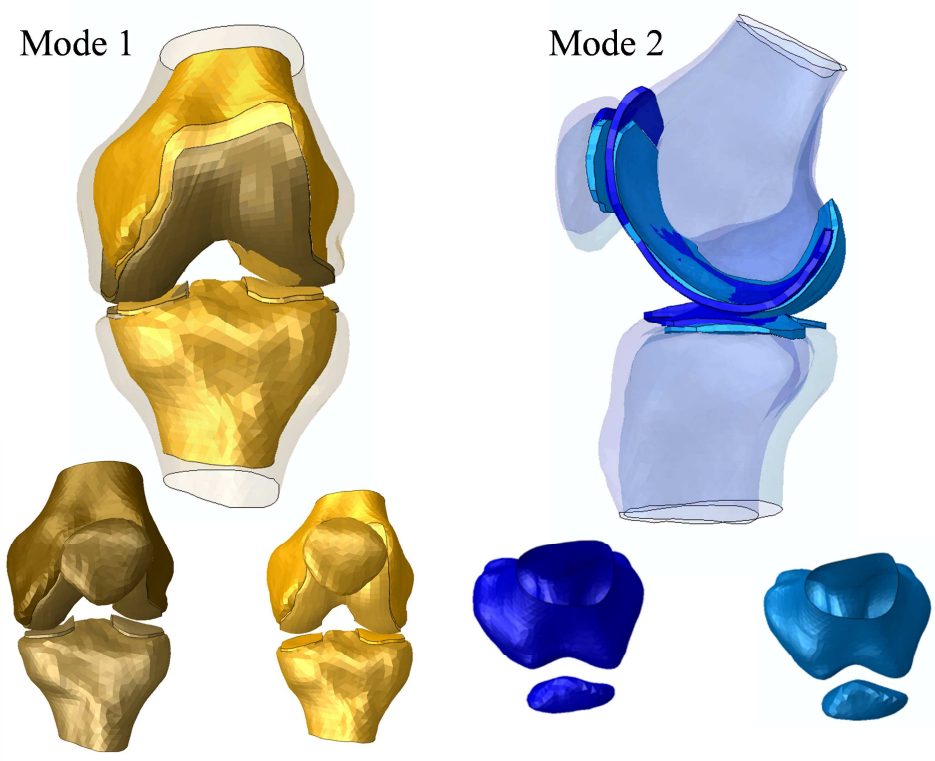

Figure 4.3: Modes of variation (1 and 2) for the statistical shape and alignment model shown at +/- 2 standard deviations. Mode 1 captured scaling in size as well as patella alta-baja. Mode 2 showing variability captured for tibial AP alignment, shape and IE alignment of the patellofemoral joint.

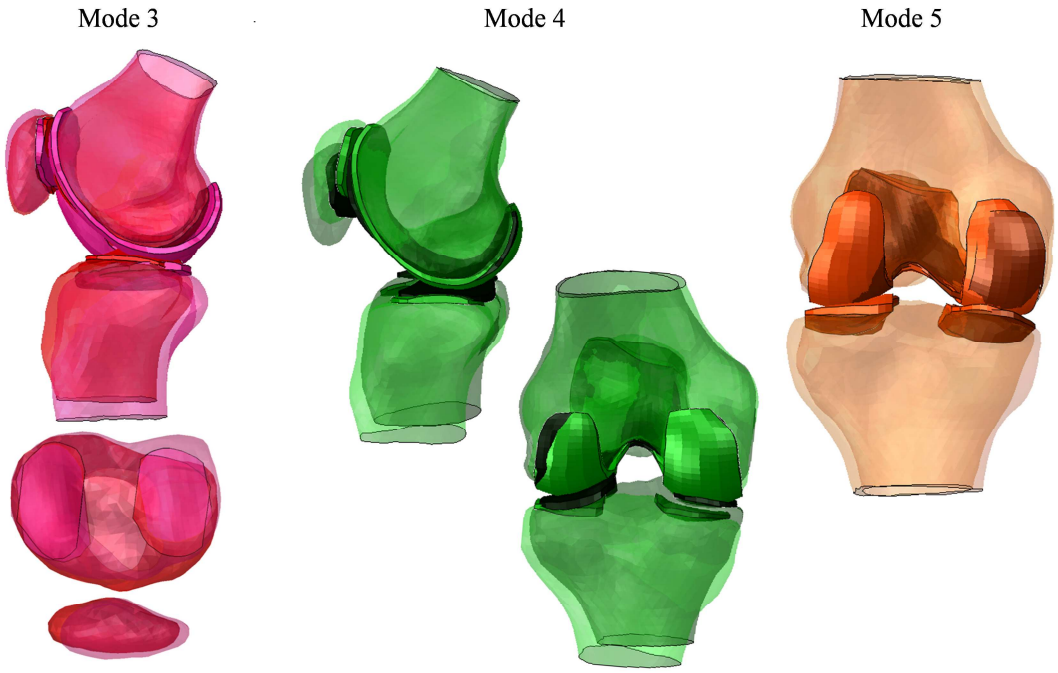

Figure 4.4: Modes of variation (3, 4 and 5) for the statistical shape and alignment model shown at +/- 2 standard deviations. Mode 3 primarily captured tibial IE rotation, Mode 4 captured patella alta-baja and tibial VV rotation, and Mode 5 captured ML width of femoral and tibial cartilages.

Table 4.3: Bone Plus Cartilages Plus Ligaments Attachment Points: Cumulative variability explained and description of characterized behavior for the most significant modes of variation.

Mode	Cumulative variability explained (Percent)	Mode Characteristics
1	20.06	scaling, patellar alta-baja
2	35.9	tibial AP translation, shape and IE rotation of the patellofemoral joint
3	47.24	Tibial IE rotation, patellar shape (medial-lateral facet ratio)

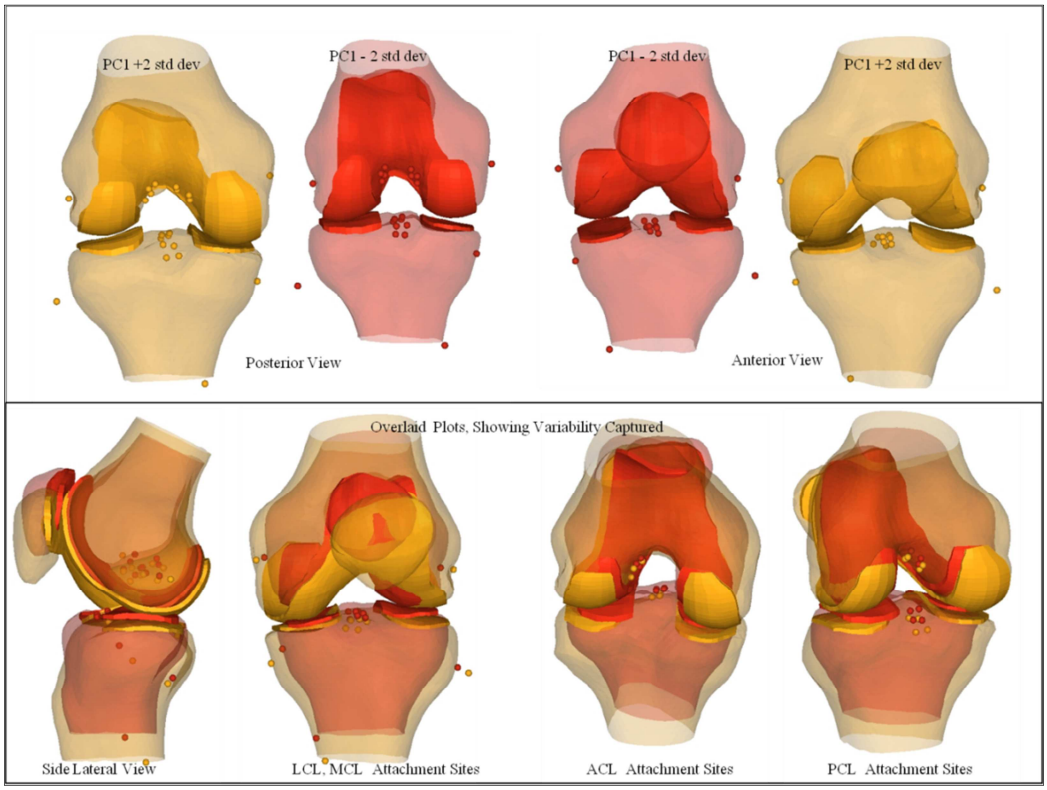

Figure 4.5: Mode 1 of the statistical shape and alignment model shown at +/- 2 standard deviations.

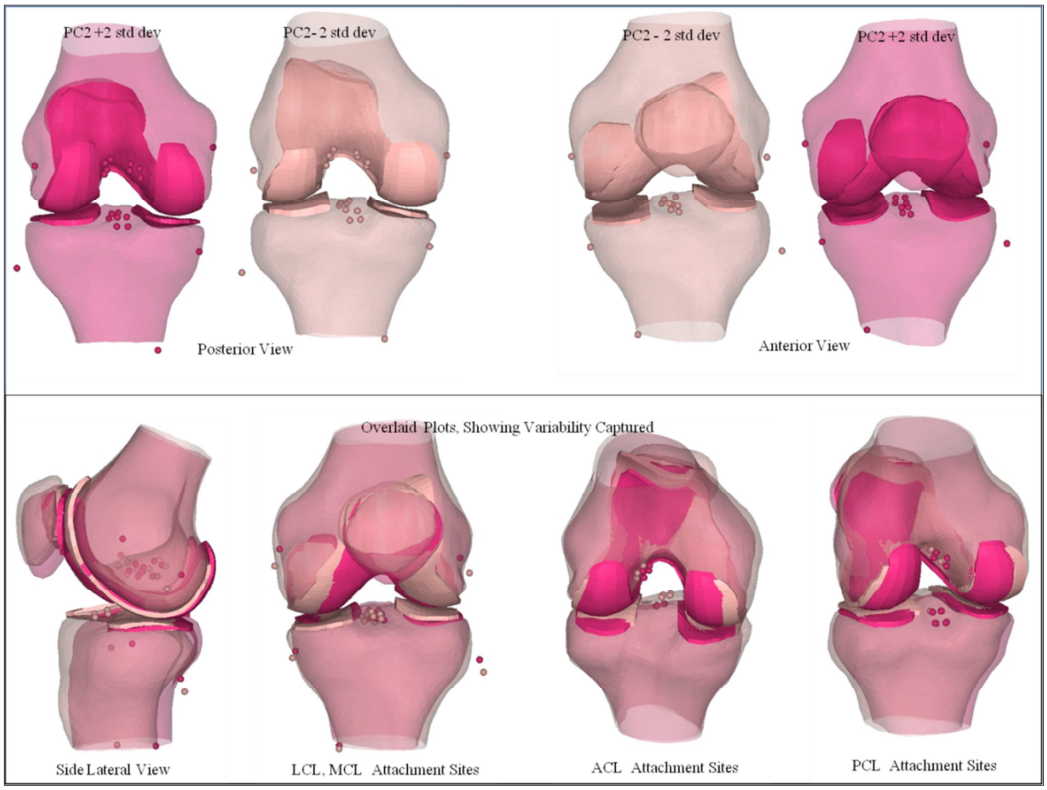

Figure 4.6: Mode 2 of the statistical shape and alignment model shown at +/- 2 standard deviations.

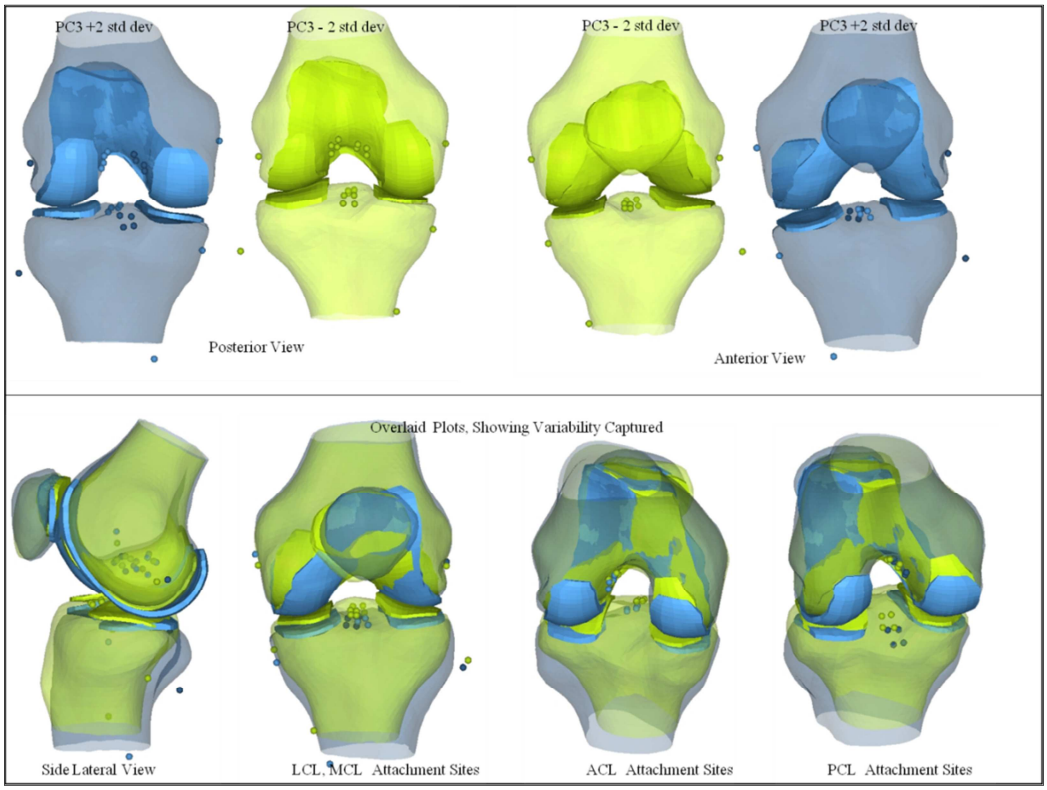

Figure 4.7: Mode 3 of the statistical shape and alignment model shown at +/- 2 standard deviations.

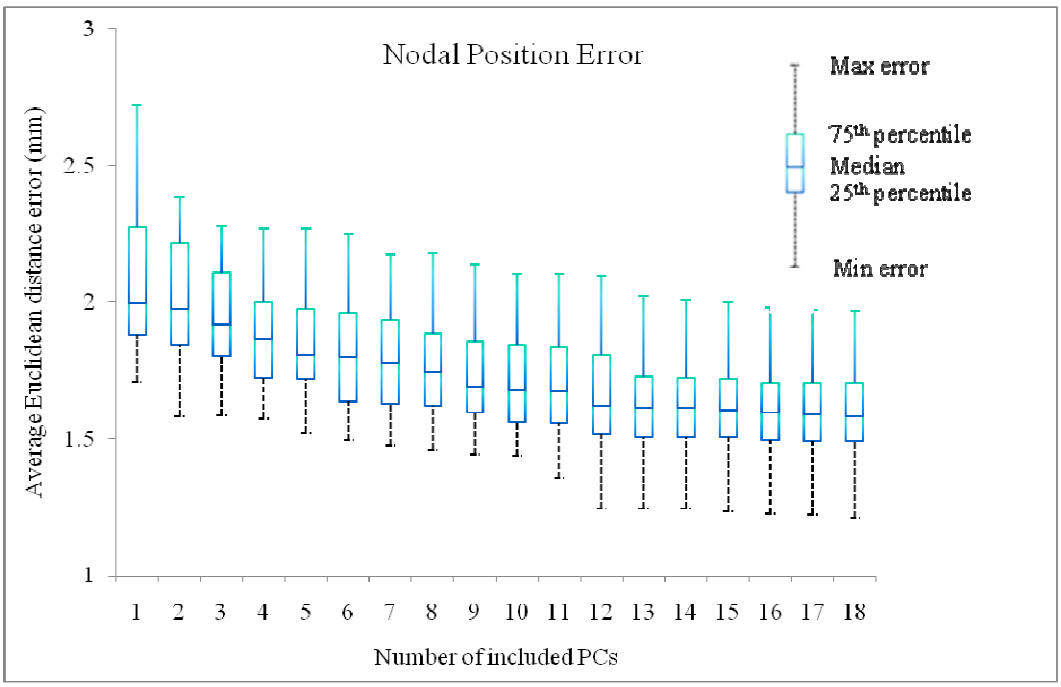

Figure 4.8: Box plots for the mean Euclidean distance error and inter-quartile range between model predicted and actual geometries, evaluated in the leave one out analysis as a function of the number of modes of variation included in the model prediction. Error is computed as the distance of nodal coordinates between the left-out geometry and its model prediction. Results are shown for median, 25^{th} and 75^{th} percentiles, minimum and maximum for the series of analyses leaving out each member of the training set.

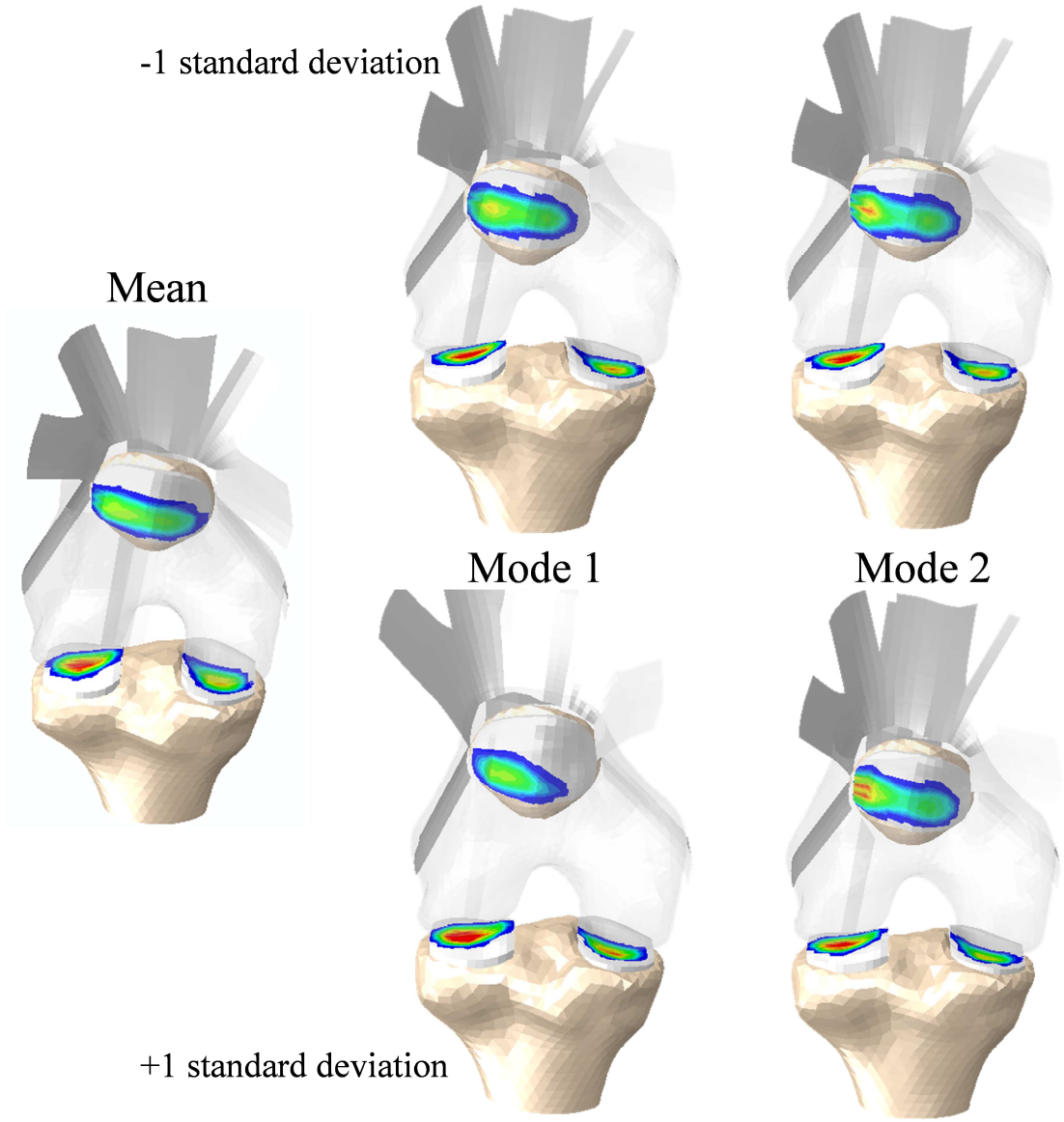

Figure 4.9: Tibiofemoral and patellofemoral contact mechanics shown for mean and ±1 standard deviation for modes 1 and 2 (Assisted by Azhar Ali, Computational Biomechanics Lab, University of Denver).

CHAPTER 5 – RELATIONSHIP BETWEEN SHAPE AND FUNCTION

5.1 Introduction

Prior statistical shape models have investigated multiple structures in a joint for shape and alignment [Rao et al., 2012; Baldwin et al., 2010; Bredbenner et al., 2010] that are required to further investigate joint mechanics for the success of the knee replacement. Also, previous studies have investigated relationships between shape of the articular geometry and joint mechanics, but have not investigated complete knee joint mechanics. Accordingly, the objective of this study was to use the statistical shape models, developed from magnetic resonance (MR) images and simulator test data, and include the kinematic variability of the same knees, and demonstrate the ability to generate realistic instances for kinematic prediction for the use in finite element analysis. Specifically, the study performed principal component analyses on training set data consisting of shape, alignment, and experimentally measured knee joint kinematics, and generated the statistical *shape-function* model.

5.2 Methods

The shape-function model was created with the shape and alignment model, and with tibiofemoral (TF) and patellofemoral (PF) kinematics. Initially, a statistical shape

and alignment was created from 20 cadaveric specimens. They were the same subjects used in the shape and alignment model (SSAM).

Digitized points represented these knee joint structures- bones:- femur, tibia, and patella, cartilages:- femoral, tibial-medial, tibial-lateral, and patellar, ligaments:- attachment points of MCL, LCL, PCL, and ACL were considered structures for each knee in the training set.

Relative alignment was done for the known flexion angle of 15^0 by aligning the knee structures to the probed points of the Kansas knee simulator (KKS). Local anatomic coordinate systems of each bone were used to derive transformation matrices for relative alignment; the positions of the tibial and patellar coordinate systems were relative to the femoral coordinate system in the KKS.

Utilizing the digitized points of knee structures and the transformation matrices in principal component analysis, each member of the training set was represented by a series of principal component (PC) scores that defined the structures.

In the KKS experiment, the cadaveric specimen was subjected to a deep knee bend loading condition and the 6 degree-of-freedom of TF and PF kinematics were measured [Baldwin et al., 2009]. Kinematic data of all the subjects were normalized from 0 to 100% cycle time and discretized into a fixed number of points (51 points) for each degree of freedom.

To develop the relationships between shape and function, a second principal component analysis was performed to create the *statistical shape-function model* using the PC shape representation and kinematic data for the training set. The size of input

matrix for second principal component was 531 x 20. It consisted of PC information data (19x20, principal components of each member of the training set) from the shape and alignment model and kinematic data (TF kinematics: 306 points, 51 x 6 dof and PF kinematics: 306 points, 51 x 6 dof).

5.3 Results

The statistical shape-function model of the knee characterized the common modes of variation with the first 3 modes representing 42.7% of the variability and 15 modes representing 95%. Anatomic (shape and alignment) variability captured by first three modes with +/- 2 std. dev. is shown is Figure 5.1. This statistical model detected the differences in the alignment which influences the motion throughout the cycle.

Shape and alignment modes were in strong agreement with the function modes. Shape figures presented to describe the anatomical variability have no ligament attachment points to simply avoid cumbersome pictures and obtain a better understanding of the shape-function relationship.

Mode 1 represented 16.6% of the variability in the shape-function combined model. The shape and alignment model captured scaling of the structures with varus-valgus (VV) rotational and medial-lateral (ML) translational alignment. The shape model was created for 15^0 flexion position. Corresponding to the same flexion angle on the kinematic (function) plot, a strong correlation between shape and function was observed. Figure 5.2 and 5.3 describe the shape and alignment model by perturbing modes with +/2 std. dev. As seen in the picture, TF- VV, TF- and PF- ML have been captured by the first

mode and the function (Figure 5.8) establishes correlated relationship with the shape model.

Mode 2 (14.4%) described relationships between TF- anterior-posterior (AP) position (Figure 5.4) and TF- AP translation (Figure 5.8); an anterior femoral position resulted in more posterior femoral translation. This mode also captured highest TF-internal-external rotation (IE) of all three modes (Figure 5.4) and the function (Figure 5.8) predicted the same. In addition, in Mode 2, a lower (baja) patella experienced greater flexion and lesser anterior translation during the cycle (Figure 5.5).

Mode 3 (11.7%) described changes in TF- AP translation (Figure 5.6) and PF-VV rotation (Figure 5.7) which were strongly supported by kinematic functions (Figure 5.8 and 5.9). As in, mode 3 in function plots predicted high AP translation (close to mode 2) of TF joints and highest VV rotation for PF joint.

5.4 Discussion

The framework for the shape-function model has been demonstrated in this study. The shape model was integrated with the joint kinematics (functions) and kinematics of the new virtual subject was predicted. In this piece of study, a statistical approach was developed to quantify the relationship between shape, alignment and kinematics. To quantify the relationship between shape and function, a second principal component analysis was performed using PC shape representation and kinematic data of the same knees obtained during deep knee bend activity in the simulator. The use of cadaveric simulator data has advantages over prior efforts. The kinematic data used are direct

measurements and accounts for the intersubject variability in anatomy, soft tissues constraint and material properties.

The shape-function model of the knee characterized the common modes of variation with the first 3 modes representing 42.7% of the variability and 15 modes representing 95%. The initial first three modes were investigated and it was found that the shape and alignment modes were in strong agreement with the function modes. It also highlighted the interdependencies between TF and PF kinematics.

The developed framework has the ability to capture the influences of complex anatomical shape and alignment in predicting the kinematic behavior.

Table 5.1: The shape and function statistical model: cumulative variability with description of characterized behavior for the first three modes of variation.

Mode	Cumulative variability explained (Percent)	Shape and alignment characteristics	Kinematic characteristics
1	16.6	Scaling, tibiofemoral patellofemoral VV rotation and ML translation	Mode 1 has highest ML translation and also VV rotation
2	31.1	Tibiofemoral IE rotation, patella alta-baja	Mode 2 has greatest TF- IE rotation and also AP translations resulting obvious alta-baja
3	42.7	Tibia AP translation and patella VV rotations	Mode3 has largest VV rotation and also AP translation

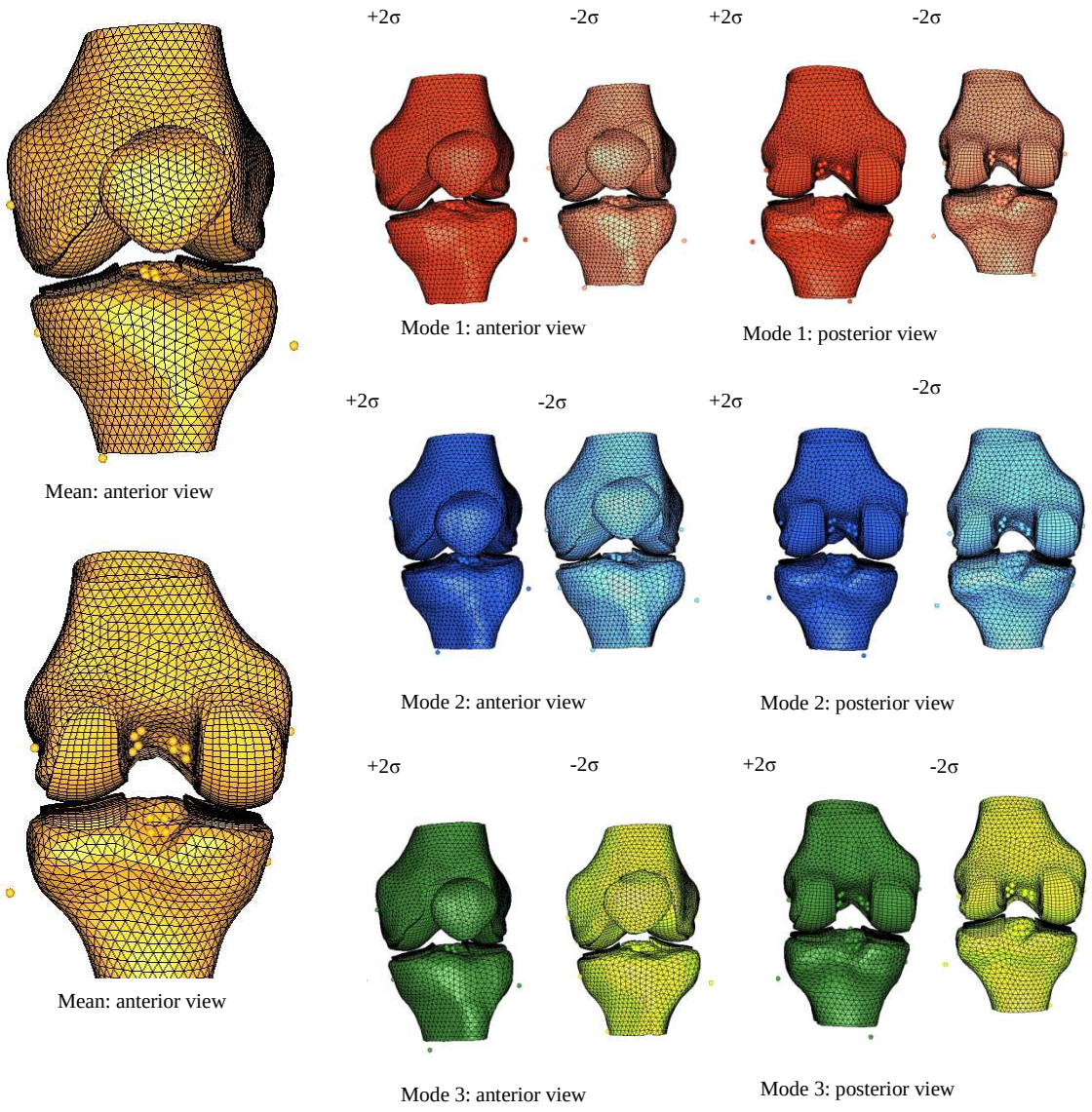

Figure 5.1: Statistical shape and alignment model showing mean and first three modes at +/- 2 standard deviations.

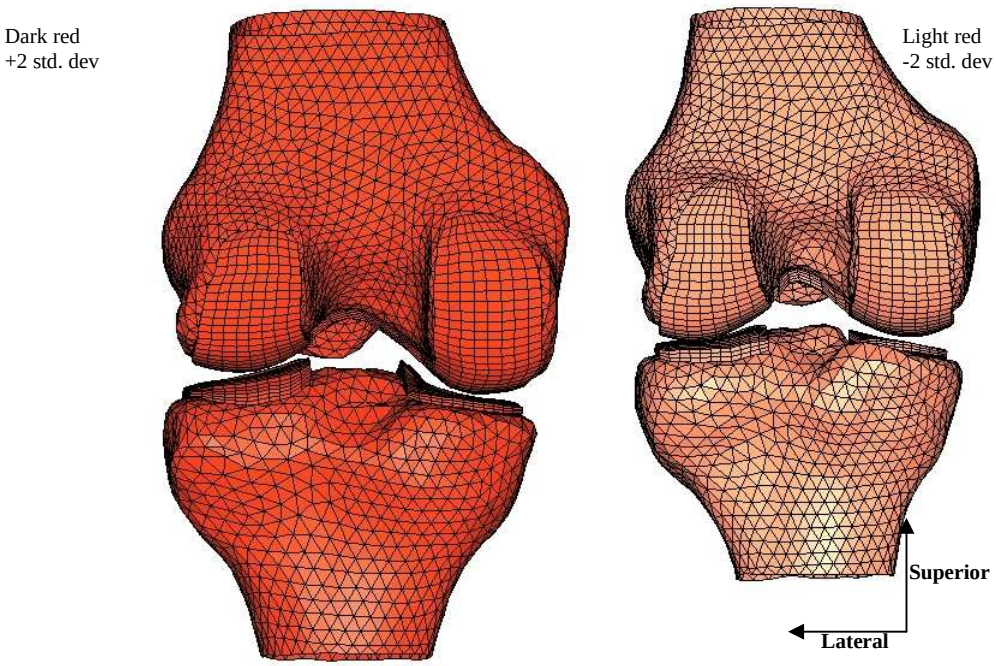

Figure 5.2: Results of the shape and alignment statistical model showing Mode 1 at +/- 2 standard deviations to describe the scaling in size and varus-valgus (one side gap between femoral and tibial cartilages).

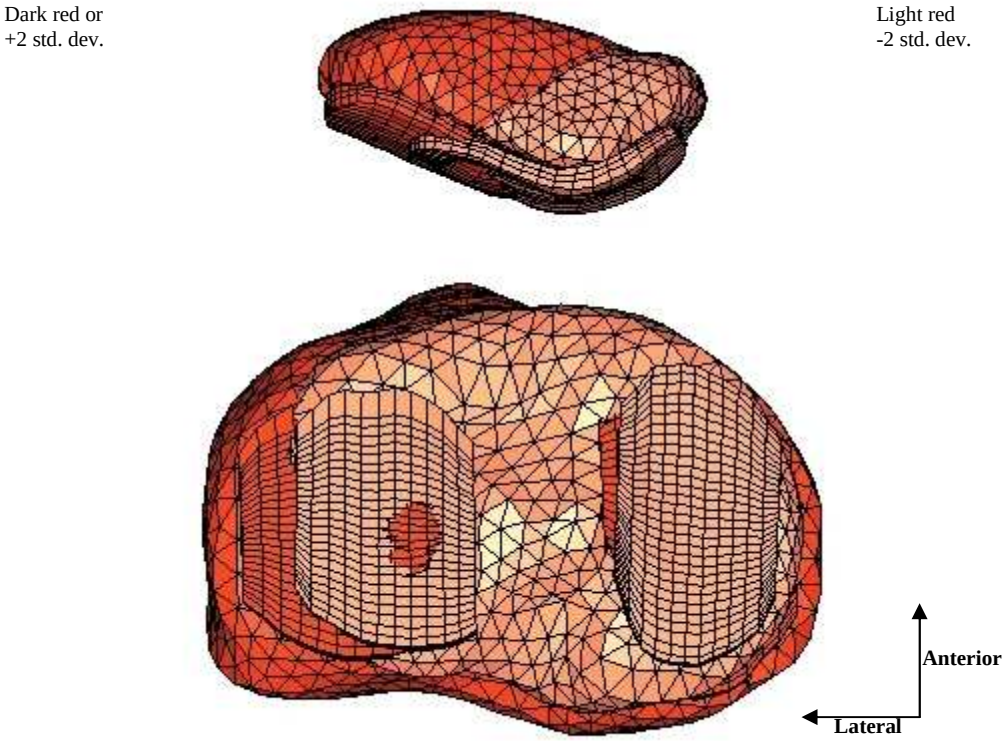

Figure 5.3: Results of the shape and alignment statistical model showing Mode 1 at +/- 2 standard deviations to describe the medial-lateral translational variability captured.

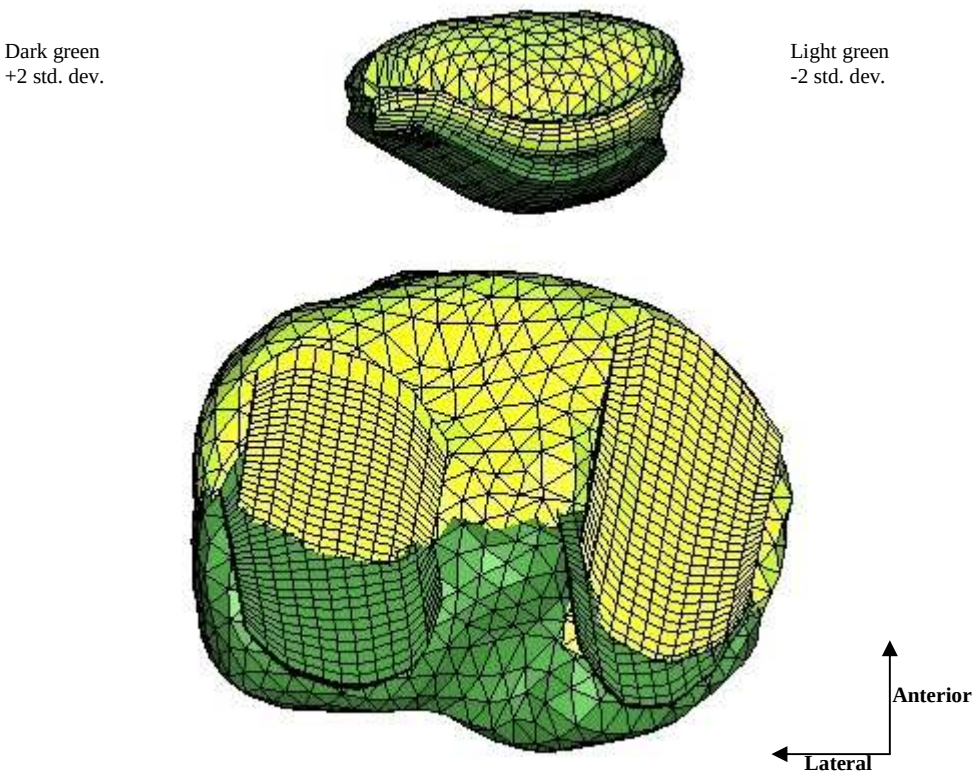

Figure 5.4: Results of the shape and alignment statistical model showing Mode 2 at +/- 2 standard deviations to describe the internal-external rotational variability captured.

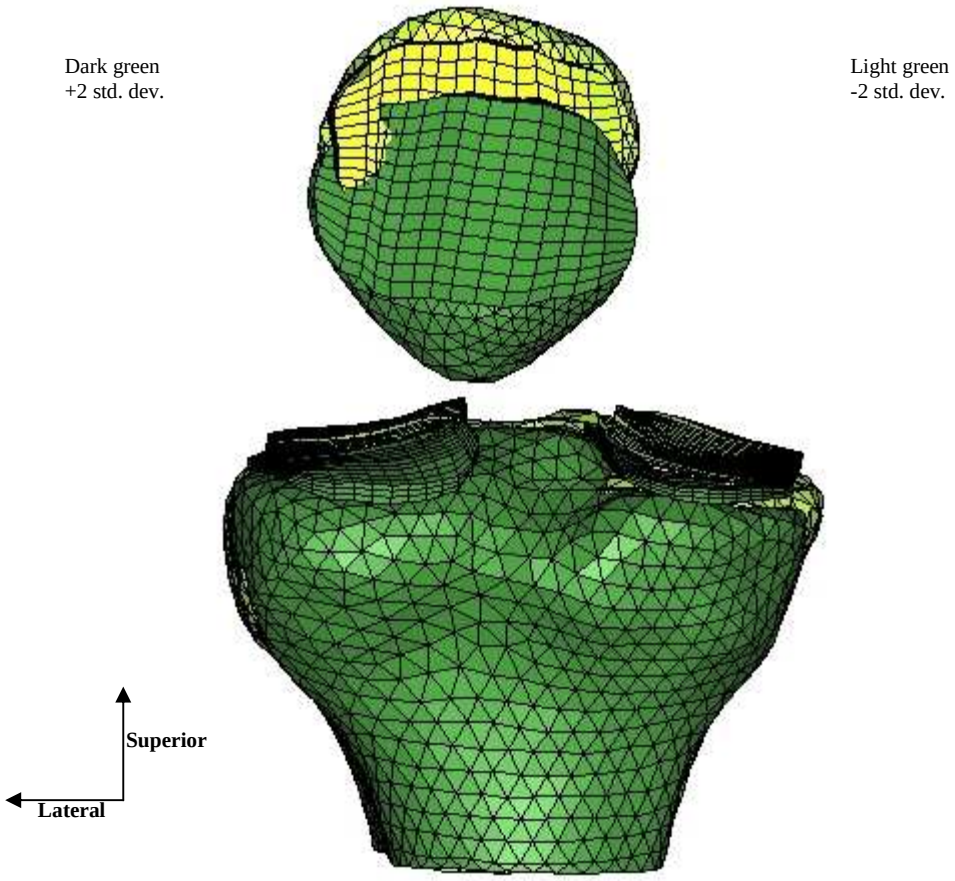

Figure 5.5: Results of the shape and alignment statistical model showing Mode 2 at +/- 2 standard deviations to describe variability captured for patella alta-baja.

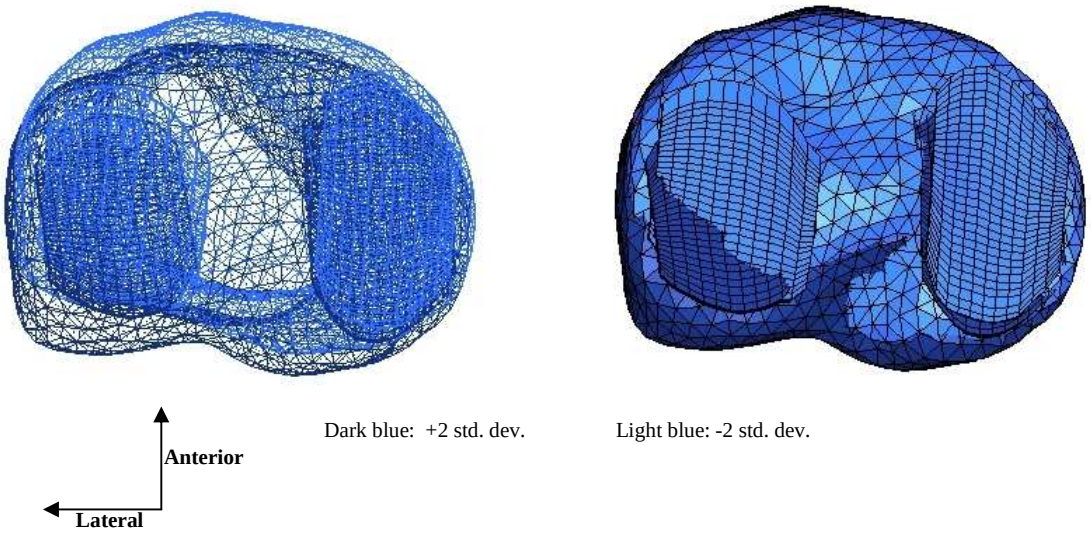

Figure 5.6: Results of the shape and alignment statistical model showing. Mode 3 at +/- 2 standard deviations to describe tibial anterior-posterior translation.

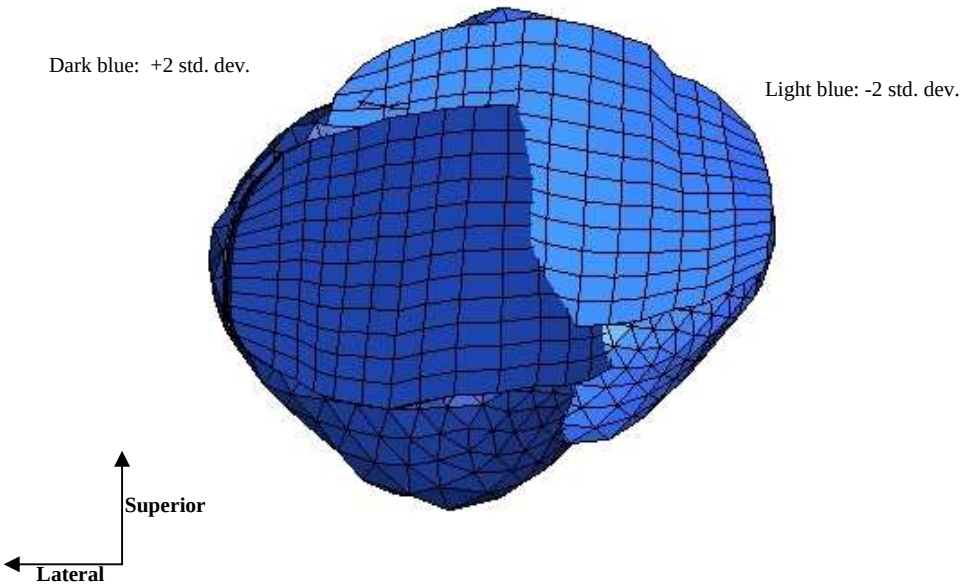

Figure 5.7: Results of the shape and alignment statistical model showing Mode 3 at +/- 2 standard deviations to describe patella medial-lateral and superior-inferior translation because of varus-valgus rotation.

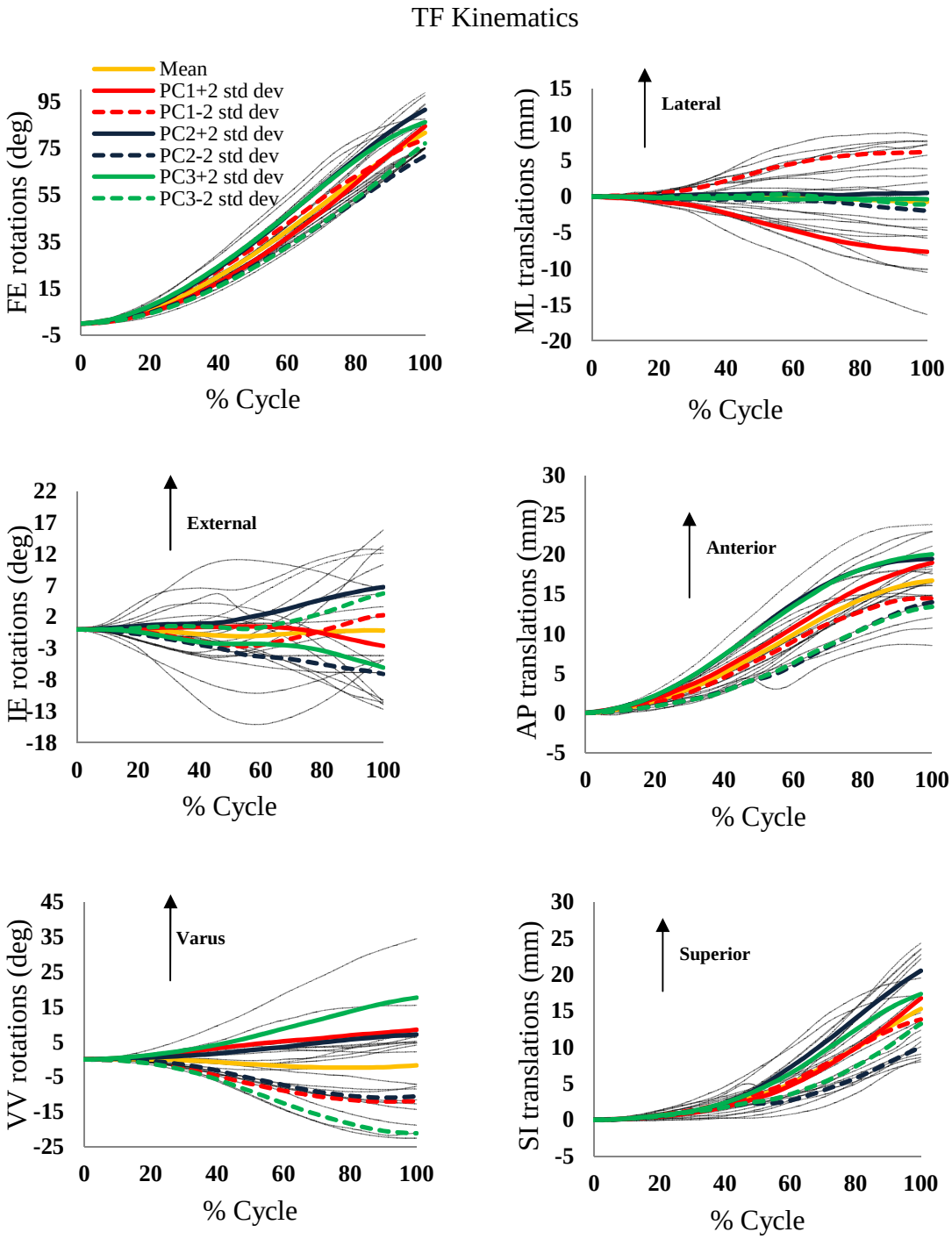

Figure 5.8: Tibiofemoral kinematics (all six dofs) shown for the first 3 principal component modes (+/-2 standard deviations) for the shape-function statistical model. Gray lines show data for all members of the training set.

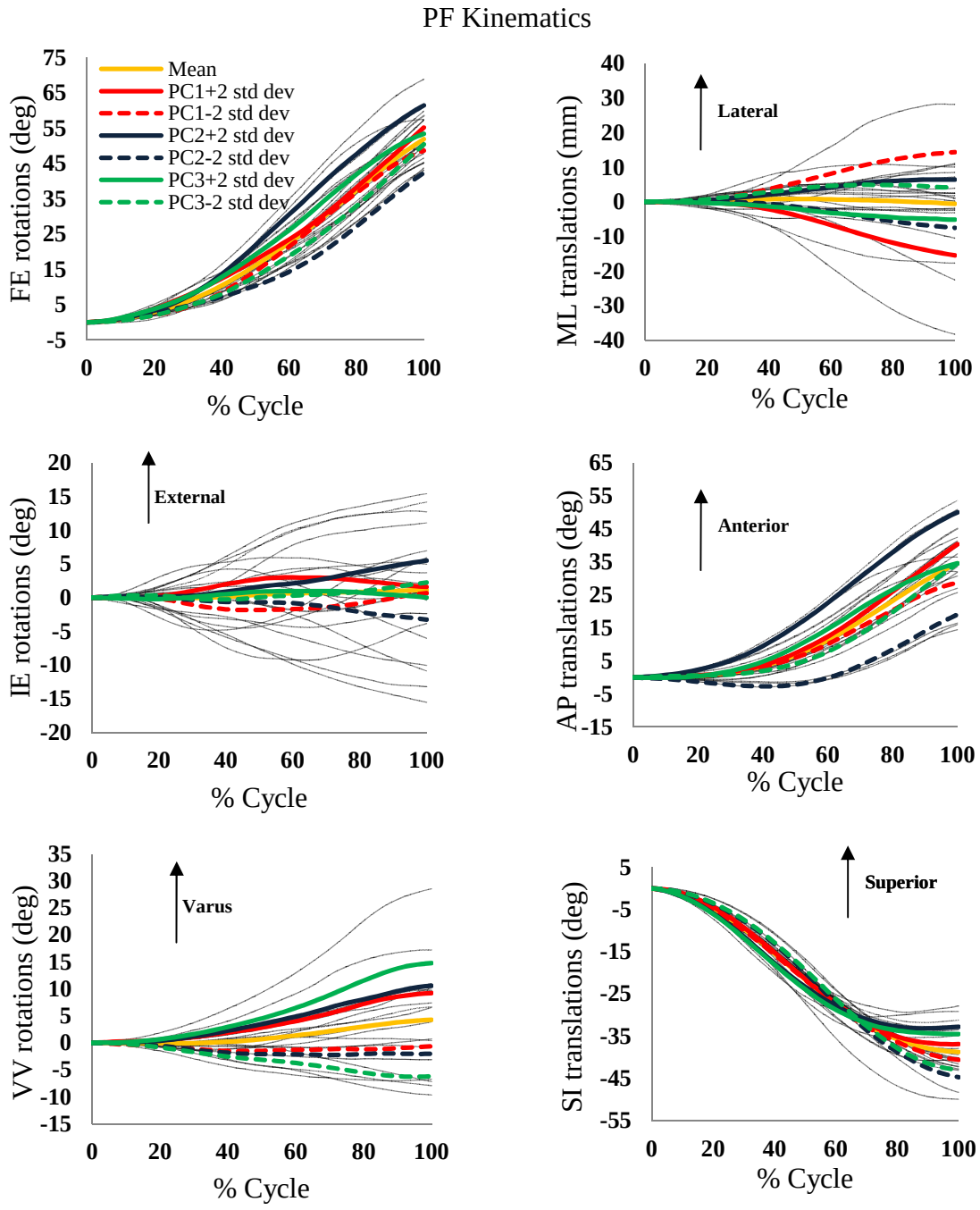

Figure 5.9: Patellofemoral kinematics (all six dofs) shown with perturbations for the first 3 principal component modes (+/-2 standard deviations) for the shape-function statistical model. Gray lines show data for all members of the training.

CHAPTER 6 – CONCLUSION

This study developed a methodological approach for statistical shape modeling of the knee joint to represent shape and alignment variability. The shape of the knee was described relative to the local anatomic coordinate system for each structure while alignment between the structures was determined at a controlled, known position. This approach enabled the development of new virtual subjects for finite element analysis use in joint mechanics assessment. The statistical model characterized the interdependencies between shape and alignment of the articular surfaces. The interdependencies characterization was important to assessing relationships between shape, alignment and kinematics and was studied through the statistical shape-function model. The shape-function model characterized the interdependencies between TF and PF kinematics.

The demonstrated workflow to generate a virtual subject from the statistical model has a variety of applications in population-based studies. As demonstrated, the shape model can contribute in joint mechanics evaluation and help in implant designs. The shape model can be helpful in subject-specific sizing of implant line based on the geometry described by it. Most current evaluations of implant designs are based on a small number of subject-specific models [Martelli et al., 2012]. Since the performance of

orthopaedic implants varies dramatically between subjects because of natural intersubject variability and surgical skill, an integrated framework will enable probabilistic analyses to assess the robustness of an implant design to patient and surgical alignment variability. The developed framework has the ability to capture the influences of complex anatomical shape and alignment in predicting the kinematic behavior. This statistical model can also be useful to investigate differences in the shape-function relationship between healthy, normal and pathologic groups (e.g. patellar maltrackers).

The availability of the simulator test data limited a smaller training set of only male population. The recommended future work includes growing the training set to include males and females to better represent population and using same workflow to develop the statistical model. As the knee anatomy has been represented in the format of finite element mesh, performing finite element analysis to predict knee mechanics could be another potential future work. Also, the development of an approach to predict virtual subjects based on anatomical landmark points will be useful in patient-specific surgical planning and robust customized implant design.

LIST OF REFRENNCES

Armstrong, A.D., Brien, H.J.C., Dunning, C.E., King, G.J.W, Johnson, J.A., Chess, D.G, 2003, Patellar position after total knee arthroplasty influence of femoral component malposition. *The Journal of Arthroplasty* Vol. 18 No. 4 458-465.

Baldwin, M.A., Langenderfer, J.E., Rullkoetter, P.J., and Laz, P.J., 2010, Development of subject-specific and statistical shape models of the knee using an efficient segmentation and mesh morphing approach. *Computer Methods and Programs in Biomedicine* 97: 232-240.

Baldwin, M.A., Clary, C., Maletsky L.P., Rullkoetter, P.J., 2009, Verification of predicted specimen-specific natural and implanted patellofemoral kinematics during simulated deep knee bend. *Journal of Biomechnics* Vol. 42, 2341-2348.

Barratt, D.C., Chan, C.S.K., Edwards, P.J., Penney, G.P., Slomczykowski, M., Carter, T.J., and Hawkes, D.J., 2008, Instantiation and registration of statistical shape models of the femur and pelvis using 3D ultrasound imaging. *Medical Image Analysis* 12(3): 358-374.

Behiels, G., Maes, F., Vandermeulen, D., and Suetens, P., 2002, Evaluation of image features and search strategies for segmentation of bone structures in radiographs using Active Shape Models. *Medical Image Analysis*, 6(1), 47-62.

Besl, P.J., McKay N.D., 1992, A method for registration of 3-D shapes. *IEEE Transactions on pattern Analysis and Machine Intelligence* 14(2), 239-256.

Bredbenner, T.L., Eliason, T.D., Potter, R.S., Mason, R.L., Havill, L.M., Nicolella, D.P. 2010, Statistical shape modelling describes variation in tibia and femur surface geometry between Control and Incidence groups from the Osteoarthritis Initiative database. *Journal of Biomechanics* 43:1780-1786.

Bredbenner, T.L. and Nicolella, D.P., 2008, Statistical Shape and Density Based Finite Element Modeling of the Human Proximal Femur. *Transactions of the 33rd Annual Meeting of the Orthopaedic Research Society*, San Francisco, CA, 0305.

Bryan, R., Mohan, P.S., Hopkins, A., Galloway, F., Taylor, M., Nair, P.B., 2010, Statistical modelling of the whole human femur incorporating geometric and material properties. *Medical Engineering and Physics* 32, 57–65.

Bryan, R., Nair, P.B., and Taylor, M., 2009, Use of a statistical model of the whole femur in a large scale, multi-model study of femoral neck fracture risk. *Journal of Biomechanics* 42, 2171–2176.

Cootes, T.F., Taylor, C.J., Cooper, D.H., and Graham, J., 1995, Active Shape Models - Their Training and Application.*Computer Vision and Image Understanding*, 61(1), 38-59.

Della C.U., Cappozzo, A., Kerrigan, D.C., 1999, Pelvis and lower limb anatomical landmark calibration precision and its propagation to bone geometry and joint angles. Medical and Biological Engineering and Computing, 37, 155–161.

Deluzio K.J., Wyss U.P., Zee B., Costigan P.A., Sorbie C., 1997, Principal component models of knee kinematics and kinetics: Normal vs. pathological gait patterns. Human Movement Science 16, 201-217.

Fitzpatrick, C.K., Baldwin, M.A., Clary, C.W., Wright, A., Laz, P.J., and Rullkoetter, P.J., 2012. Investigating alignment parameters affecting implanted patellofemoral mechanics. *Journal of Orthopaedic Research*30, 1167-75.

Fitzpatrick, C.K., 2007, Shape Analysis of the Resection Surfaces of the Knee in Relation to Implant Design. Ph.D. dissertation. *University College Dublin*.

Fitzpatrick, C.K., Baldwin, M.A., Laz, P.J., FitzPatrick, D.P., Lerner, A., and Rullkoetter, P.J., 2011. Development of a Statistical Shape Model of the Patellofemoral Joint for Investigating Relationships between Shape and Function. Journal *of Biomechanics*, Vol. 44, 2446-2452.

Fitzpatrick, C.K., Baldwin, M.A., Rullkoetter, P.J. and Laz, P.J., 2011, Coupled probabilistic and principal component analysis approach to evaluate TKR patellofemoral mechanics. *Journal of Biomechanics,* Vol. 44, 13-21.

Fitzpatrick C.K., FitzPatrick D.P., Auger D.D., 2008, Size and shape of the resection surface geometry of the osteoarthritic knee in relation to total knee replacement design. *Proc. Inst. Mech. Eng. H.* 222(6), 923-932.

Fitzpatrick, C., FitzPatrick, D., Lee, J., and Auger, D., 2007, Statistical design of unicompartmental tibial implants and comparison with current devices. *The Knee*, 14(2), 138-144.

Fritscher, K., Grunerbl, A., Hanni, M., Suhm, N., Hengg, C., Schubert, R., 2009, Trabecular bone analysis in CT and X-ray images of the proximal femur for the

assessment of local bone quality. *IEEE Transactions on Medical Imaging* 28: 1560-1575.

Galloway F., 2012, Large scale population based finite element analysis of cementless tibial tray fixation. Ph.D. dissertation. *University of Southampton*.

Harner, C. D., Baek, G.H., Vogrin, T. M., Carlin, G. J., Kashiwaguchi. S., and Woo, S. L., 1999, Quantitative analysis of human cruciate ligament insertions Arthroscopy : *the journal of arthroscopic & related surgery* : official publication of the Arthroscopy Association of North America and the International Arthroscopy Association 15 (7): 741-749.

Jolliffe, I.T., 2002, *Principal Component Analysis*. 2nd ed. Springer Series in Statistics. New York: Springer-Verlag.

LaPrade, R.F., Engebretsen, A.H., Ly, T.V., Johansen, S., Wentorf, F.A., Engebretsen, L., 2007. The Anatomy of the Medial Part of the Knee. *The Journal of Bone and Joint Surgery*, 89:2000-2010.

Laz, P.J., Browne, M., 2010, A Review of Probabilistic Analysis in Orthopaedic Biomechanics. Proceedings of the Institution of Mechanical Engineers, Part H. *Journal of Engineering in Medicine*, invited review, Vol. 224, 927-943.

Meller, S. and Kalender, W.A., 2004, Building a statistical shape model of the pelvis. *International Congress Series*, 1268, 561-566.

Martelli, S., Taddei, F., Schileo, E., Cristofolini, L., Rushton, N., Viceconti, M., 2012, Biomechanical robustness of a new proximal epiphyseal hip replacement to patient variability and surgical uncertainties: A FE study. Medical Engineering & Physics, 34, 161-171.

Mesfar, W., Shirazi-Adl, A., 2005, Biomechanics of the knee joint in flexion under various quadriceps forces. *Knee* 12, 424–434.

Morton, N.A., Maletsky, L.P., Pal, S., Laz, P.J., 2007, Effect of Anatomical Landmark Location on Knee Kinematic Description. *Journal of Orthopaedic Research* 25:1221-1230.

Pal S., 2008, Explicit Finite Element Modeling of Joint Mechanics. Ph.D. dissertation. *University of Denver*.

Pandy, M.G., Sasaki, K., Kim, S., 1997, A Three-Dimensional Musculoskeletal Model of the Human Knee Joint. Part 1: Theoretical Construction. *Computer Methods in Biomechanics and Biomedical Engineering*1:87-108.

Rajamani, K.T., Styner, M.A., Talib, H., Zheng, G., Nolte, L.P., and Gonzalez Ballester, M.A., 2007, Statistical deformable bone models for robust 3D surface extrapolation from sparse data. *Medical Image Analysis*, 11(2), 99-109.

Rao, C., Deacy, J.S., Kaschinske, S., Fitzpatrick C.K., Maletsky, L.P., Rullkoetter, P.J., Laz, P.J., 2012, Representing Intersubject Variability with a Statistical Shape and Alignment Model of the Knee. *58th Annual Meeting of the Orthopaedic Research Society*, San Francisco, CA, February 4-7, 2012.

Raychaudhuri, S., Stuart, J.M., Altman, R.B., 2000, Principal components analysis to summarize microarray experiments: application to sporulation time series. *Pacific Symposiuum on Biocomputing* 5:452-463.

Shim, V.B., Pitto, R.P., Streicher, R.M., Hunter, P.J., and Anderson, I.A., 2008, Development and validation of patient-specific finite element models of the hemipelvis generated from a sparse CT data set. *Journal of Biomechanical Engineering - Transactions of the ASME*, 130(5).

Taddei, F., Martelli, S., Reggiani, B., Cristofolini, L., Viceconti, M., 2006. Finite-Element Modeling of Bones From CT Data: Sensitivity to Geometry and Material Uncertainties. *IEEE Transactions on biomedical engineering,* VOL. 53, NO. 11.

The Osteoarthritis Initiative, a multi-center, four-year observational study of men and women. http://oai.epi-ucsf.org.

Yang, Y.M., Rueckert, D., Bull, A.M.J., 2008, Predicting the shapes of bones at a joint: application to the shoulder. *Computer Methods in Biomechanics and Biomedical Engineering*, , 11(1), 19-30.

APPENDIX A: ANATOMICAL LANDMARK POINTS FOR LOCAL COORDINATE SYSTEMS

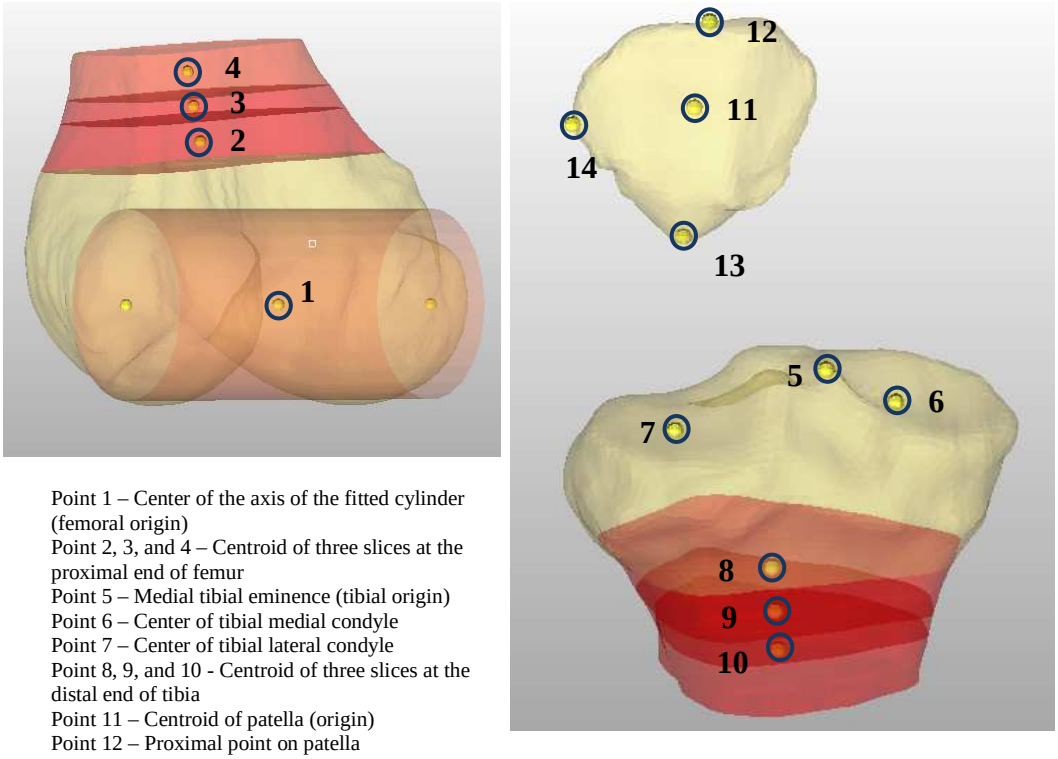

Point 1 – Center of the axis of the fitted cylinder (femoral origin)
Point 2, 3, and 4 – Centroid of three slices at the proximal end of femur
Point 5 – Medial tibial eminence (tibial origin)
Point 6 – Center of tibial medial condyle
Point 7 – Center of tibial lateral condyle
Point 8, 9, and 10 - Centroid of three slices at the distal end of tibia
Point 11 – Centroid of patella (origin)
Point 12 – Proximal point on patella
Point 13– Distal point on patella
Point 14 – Lateral point on patella

Figure A.1: Depiction of anatomical landmark points utilized for the construction of local coordinate system of each bone.

APPENDIX B: REPRESENTATION OF FEMORAL LIGAMENT ATTCHEMNT SITES BY POINTS

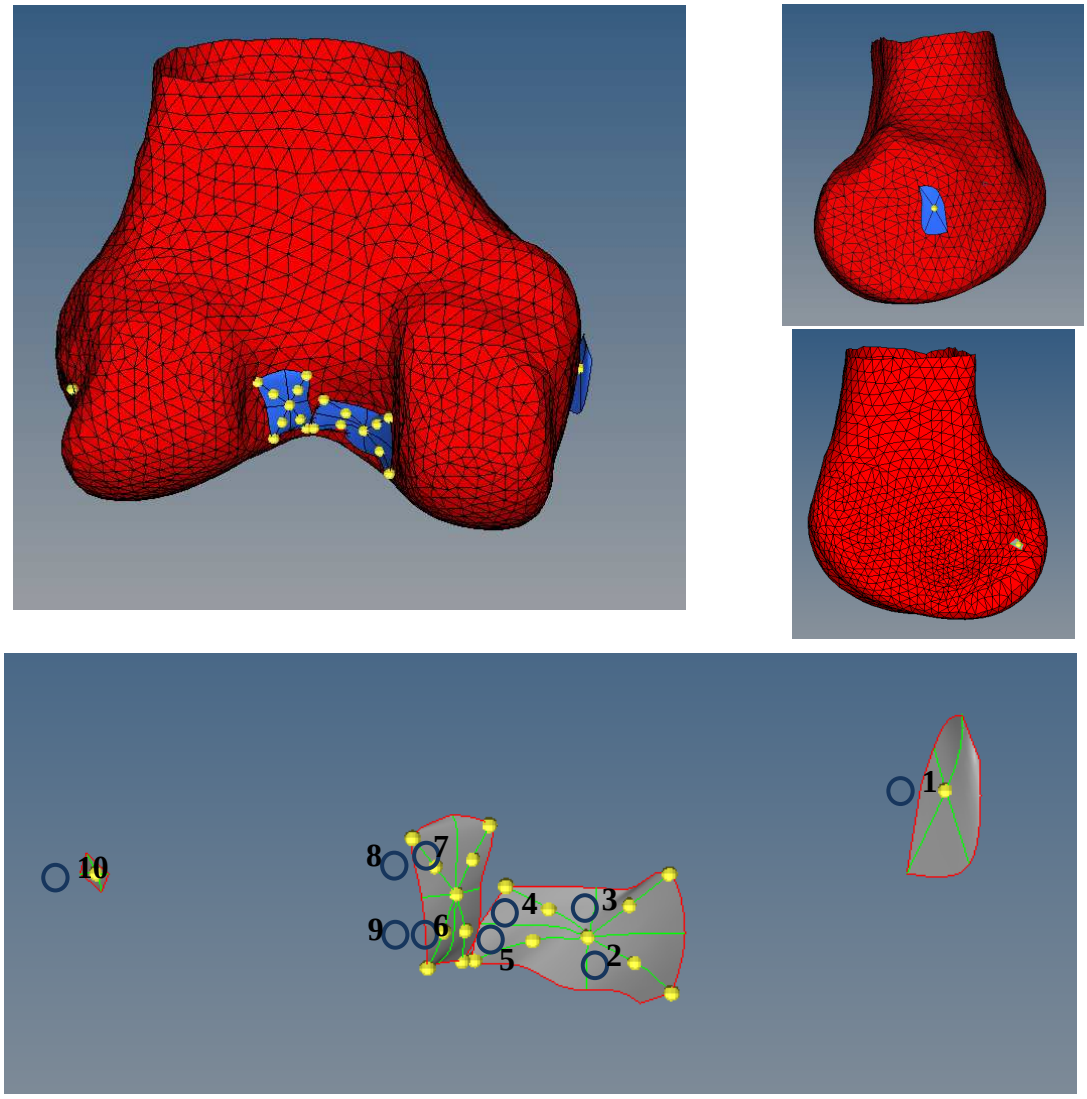

Figure B.1: For example- femoral ligament attachment point; surfaces of ligaments (from 3D constructed geometries) close to bone were extracted; ACL and PCL sites were quartered approximately and center of each diagonal (total 4 for each attachment site) was taken as an attachment point. MCL and LCL sites surface was diagonally divided and intersection of diagonals was taken as attachment point.

APPENDIX C: KINEMATIC EXTRACTION PROCESS USING TRANSFORMATION MATRICES

Main steps of relative transformation matrices development for kinematics extraction are as follows:

1. Each bone (tibia and patella) local coordinate system was reported in the femoral rigid body space.

2. Each bone's rigid body transformation matrix information was available in the global camera space *(based on KKS experimental data sheet).*

3. inv(CT0)*CF0*tibz' = Transformation of tibial local coordinate system was done in the tibial rigid body space using global camera (inv(CT0)*CF0*tibz', where CT0 is transformation matrix of tibial rigid body in camera space, CF0 is transformation matrix of femoral rigid body in camera space, tibz is tibial Z-axis). This was done for particular time point at which tibia local coordinate system was reported in the femoral rigid body space. *Fixed with time*.

4. CTf = Transformation of tibial rigid body in global camera space. *Varying in time.*

5. inv(CFf) = Transformation of global camera space with respect to femoral rigid body. *Varying in time.* Now, tibia axes information is femoral rigid body space.

6. inv(CFf)*CTf*inv(CT0)*CF0*tibz' = Transformation gave tibial axes in the femoral rigid body space. *Varying in time.*

7. Femoral axes were in already in femoral rigid body space. *Fixed.*

8. Final transformation, inverse of tibial axes information in femoral rigid body space * femoral axes in femoral rigid body space = Transformation of tibial local coordinate system to the femoral local coordinate system, and was used to calculate 6 degree of freedom. *Varying in time*.

APPENDIX D: PUBLICATIONS

Journal

- Rao, C., Fitzpatrick, C.K., Rullkoetter, P.J., Kim, R., Maletsky, L.P., Laz, P.J., "A statistical model accounting for intersubject shape and alignment variability in the knee". *Medical Engineering and Physics*, in review.

Conference

- Rao, C., Deacy, J S, Kaschinske, S, Fitzpatrick C K, Maletsky, L P, Rullkoetter, P J, Laz, P J., "Representing Intersubject Variability with Statistical Shape and Alignment Model of the Knee". *58th Annual Meeting of the Orthopaedic Research Society*, February 4-7, 2012, San Francisco, California, poster presentation.